SEVERAL PATH-FOLLOWING METHODS FOR A CLASS OF GRADIENT CONSTRAINED VARIATIONAL INEQUALITIES

M. HINTERMÜLLER AND J. RASCH

Abstract. Path-following splitting and semismooth Newton methods for solving a class of problems related to elasto-plastic material deformations are proposed, analyzed and tested numerically. While the splitting techniques result in alternating minimization schemes, which are typically linearly convergent, the proposed Moreau-Yosida regularization based semismooth Newton technique and an associated lifting step yield local superlinear convergence in function space. The lifting step accounts for the fact that the operator associated with the linear system in the Newton iteration need not be boundedly invertible (uniformly along the iterates). For devising an efficient update strategy for the path-following parameter regularity properties of the path are studied and utilized within an inexact path-following scheme for all approaches. The paper ends by a report on numerical tests of the different approaches.

Introduction

Elasto-plastic material deformation is associated with the minimization of a quadratic energy subject to pointwise constraints on the norm of the gradient of the displacement. In case the pointwise norm of the gradient equals a given plasticity threshold, then the deformation is plastic; otherwise it is elastic. Mathematically and in the context of a simple model problem, this continuum-mechanic principle is stated as

$$\text{(P)} \qquad \begin{aligned} &\text{minimize } J(y) := \frac{1}{2}\int_\Omega |\nabla y(x)|_2^2 \, dx - \int_\Omega f(x)y(x)\,dx \quad \text{over } y \in H_0^1(\Omega) \\ &\text{subject to (s.t.) } y \in M := \{z \in H_0^1(\Omega) \mid |\nabla z| \le \psi \text{ a.e. in } \Omega\}, \end{aligned}$$

where $\Omega \subset \mathbb{R}^n$ is a bounded open subset with Lipschitz boundary $\partial\Omega$, $f \in L^2(\Omega)$ represents some external loading condition and $\psi \in L^q(\Omega)$, $\psi \ge \underline{\psi} > 0$ almost everywhere (a.e.) in Ω, denotes the heterogeneous plasticity threshold. Throughout this work we assume that $q > 2$. Properties which hold up to a set of Lebesgue measure zero are stated in terms of 'a.e.', i.e., 'almost everywhere'. For the Euclidean norm in $\mathbb{R}^n$ we write $|\cdot| = |\cdot|_2$. In case of anisotropies other ℓ_r-norms, $r \in [1, +\infty]$, may appear more appropriate. While the focus here is on $r = 2$, we note, however,

2000 *Mathematics Subject Classification.* 49M15, 49M37, 65K05, 65K10, 65K15, 90C48, 90C33.

Key words and phrases. Pointwise gradient constraints, Moreau-Yosida regularization, path-following, semi-smooth Newton-methods, splitting methods.

This research was supported by the DFG Research Center Matheon through Project C28, the Einstein Center for Mathematics Berlin through projects SE5 and OT1, and the Austrian Science Fund FWF by START Project Y305 "Interfaces and Free Boundaries" as well as the DFG Project HI 1466/7-1. The authors also would like to thank T.M. Surowiec (Humboldt-Universität zu Berlin) for detailed discussions on first-order conditions and directional differentiability of the value functional.

Computers and Mathematics with Applications 69 (2015) 1045–1067
The final publication is available at Elsevier:
http://dx.doi.org/10.1016/j.camwa.2014.12.001

that the subsequent development remains true for general $r \in [1, +\infty]$. For the definition and properties of Lebesgue spaces $L^s(\Omega)$, $s \in [1, +\infty]$, and Sobolev spaces $W_0^{1,s}(\Omega)$ we refer to [1].

Gradient constrained problems were considered in the context of splitting and augmented Lagrange methods in [10]. In this context, typically a new variable, say p, is introduced and

$$(\mathrm{P}^1_\gamma) \qquad \begin{aligned} &\text{minimize } J^1_\gamma(y,p) \quad \text{over } (y,p) \in H^1_0(\Omega) \times L^2(\Omega)^n \\ &\text{s.t. } p \in M^1 := \{v \in L^2(\Omega)^n \mid |v|_2 \leq \psi \text{ a.e. in } \Omega\} \end{aligned}$$

is solved, where $\gamma > 0$ denotes a penalty parameter and

$$J^1_\gamma(y,p) := \frac{1}{2}\int_\Omega |\nabla y|_2^2 \, dx - \int_\Omega f y \, dx + \frac{\gamma}{2}\int_\Omega |\nabla y - p|_2^2 \, dx.$$

Relaxing the inequality constraints by adding the Moreau-Yosida regularization of the indicator function of M^1 to J^1_γ we arrive at

$$\begin{aligned} J^2_\gamma(y,p) := \frac{1}{2}\int_\Omega |\nabla y|_2^2 \, dx - \int_\Omega f y \, dx + \frac{\gamma}{2}\int_\Omega |\nabla y - p|_2^2 \, dx \\ + \frac{\gamma}{2}\int_\Omega \left|(|p|_2 - \psi)^+\right|_2^2 \, dx \end{aligned}$$

and consider the alternative unconstrained splitting problem

$$(\mathrm{P}^2_\gamma) \qquad \text{minimize } J^2_\gamma(y,p) \quad \text{over } (y,p) \in H^1_0(\Omega) \times L^2(\Omega)^n.$$

For both of this splitting techniques, alternating minimization schemes can be applied, i.e., keep y fixed and solve for p and vice versa until convergence. While the resulting subproblems are either explicitly or rather straight forward to solve and convergence follows from standard arguments, the overall difficulty of the problem results in a large number of iterations as can be observed, e.g., from the results in Section 5.

As a remedy to the moderate convergence behavior of splitting schemes, we propose a semismooth Newton scheme. For this purpose, we employ the Moreau-Yosida regularization of the indicator function of the constraint set M in (P). This yields

$$J^3_\gamma(y) := \frac{1}{2}\int_\Omega |\nabla y|_2^2 \, dx - \int_\Omega f y \, dx + \frac{\gamma}{2}\int_\Omega \left|(|\nabla y|_2 - \psi)^+\right|_2^2 \, dx,$$

where, again, $\gamma > 0$. Consequently, (P) is approximated by

$$(\mathrm{P}^3_\gamma) \qquad \text{minimize } J^3_\gamma(y) \quad \text{over } y \in H^1_0(\Omega).$$

Semismooth Newton methods have been successfully studied in [14, 22, 23] and the references therein in the context of optimization problems with partial differential equation constraints and variational inequality problems. They exhibit fast local convergence and, once successfully analyzed in function space, a mesh independent convergence [20].

In the context of elastic perfectly plastic material behavior, Newton-type solvers were already considered in [8, 31]. We note that the problem formulation in these papers is in terms of the dual variables (stresses) and the pointwise constraint on the deviator of the stress is kept explicit (rather than penalized or handled by splitting). It is known [14, 13] that keeping such (state) constraints explicit and handling the associated complementarity system for characterizing solutions by means of NCP-functions yielding a nonsmooth system of equations does typically not allow for a

function space version of the generalized Newton method. As a consequence, adverse *mesh dependent convergence* may occur. For a class of elasto-plastic problems, an example for the latter can be found in [12]. Utilizing the Moreau-Yosida regularization, it was shown in [15, 13, 18] that the associated regularized problems can be solved efficiently, i.e. at a local superlinear rate, by a semismooth Newton method in function space. Then the results in [20] allow to conclude mesh independent convergence. In the present paper, we aim at such a mesh independent version of Newton's method. However, we point out that the gradient constraint complicates the analysis as it requires a lifting step after each Newton step in order to maintain a certain norm gap needed for proving semismoothness of the nonsmooth maps associated with systems to be solved.

The splitting and/or the Moreau-Yosida regularization induce a parameter dependent nonsmooth system of equations characterizing first order optimality. Consequently (and typically for other path following methods as well), in all of the above methods the handling of the parameter γ is a delicate issue in its own right. On the one hand, one would like to increase it quickly as $\gamma \to \infty$ yields that the solutions to the split-penalized and Moreau-Yosida regularized problems converge to the solution of (P), respectively. A rapid increase of γ, however, may suffer from large iteration counts when solving the respective subproblems. On the other hand, while a slow increase prevents this problem, it suffers from a large number of γ-update iterations. For the obstacle problem, tailored path-following or γ-update schemes were proposed in [15] in order to achieve a compromise between the two aforementioned extremes. Here we extend this framework to the gradient-constrained case.

We mention that path-following schemes for problems posed in function space have become popular in the recent years. Moreau-Yosida based path-following for state constraints or constraints on the gradient of the state can be found in [15, 16, 19]. For barrier type methods we refer to [26, 25, 29, 30]. While barrier methods typically aim at approaching a solution from within the feasible set, Moreau-Yosida based path-following, as considered in the present paper, allows violations of the inequality constraint associated with the underlying problem. In optimization problems with partial differential equation constraints and pointwise constraints on states and/or controls another regularization scheme, which induces a path, is of Lavrentiev type [28, 7]. Like the Moreau-Yosida regularization, the latter scheme also admits constraint violations. It appears, however, that the Lavrentiev regularization induces a more complex path-structure when compared with the Moreau-Yosida regularization, which may be disadvantageous numerically.

Notation. Throughout this paper, X^* denotes the dual space of a real Banach space X with associated duality pairing $\langle \cdot, \cdot \rangle_{X^*,X}$. Strong convergence is denoted by $\to$ whereas weak convergence is written as $\rightharpoonup$. Continuous embedding of X in Y is written as $X \hookrightarrow Y$ and compact embedding as $X \subset\subset Y$. In case X admits an inner product, then we write $(\cdot, \cdot)_X$ with induced norm $\|\cdot\|_X$. By "a.e." we mean "almost everywhere", i.e., up to a set of Lebesgue measure zero. For a closed, convex subset M of X, I_M denotes the associated indicator function, i.e., $I_M(x) := 0$ if $x \in M$ and $I_M(x) := +\infty$ otherwise. Constants $c > 0$ are normally considered to be generic, $\max(0, \cdot)$ respectively $-\min(0, \cdot)$ are often denoted by $(\cdot)^+$ respectively $(\cdot)^-$.

The rest of the paper is organized as follows. Section 1 studies the existence and uniqueness of a solution to the original and the regularized problems. Moreover, consistency results are established and first order optimality conditions are stated.

Section 2 describes the algorithms relying on the splitting technique in detail. The semismooth Newton method for solving the first order necessary and sufficient system associated with the regularized problem is given in Section 3 and the implemented algorithm is described. Moreover, in this section the necessity of lifting steps is argued and a local convergence analysis of the resulting method is given. In Section 4 we develop numerical update strategies for the penalty parameter γ using a model function. Here, the path value functionals for all three approaches are introduced and differentiability properties of these functionals are established. Exact as well as inexact path-following methods are introduced. Finally, in Section 5 we report our numerical results and compare the algorithms.

1. Several Variable Splitting Approaches

In this section, we provide a detailed analysis of the three different splitting and penalization approaches.

1.1. Existence and Uniqueness.

Existence and uniqueness of a solution y^* to (P) are immediate consequences of the $H_0^1(\Omega)$-coercivity and uniform convexity of the objective function in (P) as well as the weak closedness of the convex set M; compare [9, Prop.1.2, p.35].

Let $\gamma > 0$ be fixed. For the penalized problem (P_γ^1), we consider an infimizing sequence $\{(y_k, p_k)\}$. Since $(0, 0)$ is feasible, $\{(y_k, p_k)\}$ is uniformly bounded. Therefore $\{y_k\}$ is bounded in $H_0^1(\Omega)$ and, owing to the structure of the objective (or alternatively M^1), $\{p_k\}$ is bounded in $L^2(\Omega)^n$. Hence, there exists a weakly convergent subsequence of $\{(y_k, p_k)\}$ with limit $(y_\gamma, p_\gamma) \in H_0^1(\Omega) \times L^2(\Omega)^n$. Using the weak closedness of M^1, we have $p_\gamma \in M^1$, and since J_γ^1 is weakly lower semicontinuous, we get that (y_γ, p_γ) is a solution to (P_γ^1). Uniqueness of the solution follows from the uniform convexity of J_γ^1.

For problem (P_γ^2) and (P_γ^3) we proceed analogously to establish existence of a solution.

1.2. Consistency.

Now we investigate the relation of the solutions of the penalized problems introduced in Section 1 to the original solution y^* of (P).

Theorem 1.1 Let $\{(y_\gamma, p_\gamma)\}_{\gamma \geq 0}$ in $H_0^1(\Omega) \times L^2(\Omega)^n$ denote the path of solutions of (P_γ^1) (parametrized by γ). Then $(y_\gamma, p_\gamma) \to (y^*, \nabla y^*)$ strongly in $H_0^1(\Omega) \times L^2(\Omega)^n$ as $\gamma \to \infty$.

Proof. The optimality of (y_γ, p_γ) and feasibility of $(y^*, \nabla y^*)$ for (P_γ^1) yield

$$\frac{1}{2} \|y_\gamma\|^2_{H_0^1(\Omega)} - (f, y_\gamma)_{L^2(\Omega)} \leq J_\gamma^1(y_\gamma, p_\gamma) \leq J_\gamma^1(y^*, \nabla y^*) = J(y^*) \quad \forall \gamma. \tag{1.1}$$

Thus, by coercivity of J with respect to y, we have that $\{y_\gamma\}$ is bounded in $H_0^1(\Omega)$. From $\{p_\gamma\} \subset M^1$ we infer the existence of a subsequence $(y_{\gamma'}, p_{\gamma'}) \rightharpoonup (\bar{y}, \bar{p})$ in $H_0^1(\Omega) \times L^2(\Omega)^n$ as $\gamma' \to \infty$. The weak closedness of M^1 yields $\bar{p} \in M^1$. This fact, the weak lower semicontinuity of J and (1.1) imply

$$J(y^*) \overset{(1.1)}{\geq} \liminf_{\gamma \to \infty} \frac{1}{2} \|y_\gamma\|^2_{H_0^1(\Omega)} - (f, y_\gamma)_{L^2(\Omega)} \geq J(\bar{y}).$$

It remains to show that $\bar{y}$ is feasible, i.e. $\bar{y} \in M$. Since

$$\frac{\gamma}{2}\,\|\nabla y_\gamma - p_\gamma\|^2_{L^2(\Omega)^n} - \|f\|_{L^2(\Omega)}\,\|y_\gamma\|_{L^2(\Omega)} \le J^1_\gamma(y_\gamma, p_\gamma) \le J^1_\gamma(y^*, \nabla y^*) = J(y^*) \quad \forall\gamma$$

and $\{y_\gamma\}$ is bounded, we get $\|\nabla y_\gamma - p_\gamma\|_{L^2(\Omega)^n} \to 0$ for $\gamma \to \infty$. Using the weak lower semicontinuity of $\|\cdot\|^2_{L^2(\Omega)^n}$, we have

$$0 = \liminf_{\gamma\to\infty} \|\nabla y_{\gamma'} - p_{\gamma'}\|^2_{L^2(\Omega)^n} \ge \|\nabla\bar{y} - \bar{p}\|^2_{L^2(\Omega)^n}\,.$$

This leads to $\bar{p} = \nabla\bar{y} \in M^1$ and by uniqueness of the solution we have $\bar{y} = y^*$. By uniqueness, all weakly converging subsequences have the same limit. Hence, the whole sequence $\{(y_\gamma, p_\gamma)\}$ converges weakly to $(y^*, \nabla y^*)$.

Next observe that

$$\begin{aligned}\frac{1}{2}\|y^*\|^2_{H^1_0(\Omega)} &\le \liminf_\gamma \frac{1}{2}\|y_\gamma\|^2_{H^1_0(\Omega)} \le \limsup_\gamma \frac{1}{2}\|y_\gamma\|^2_{H^1_0(\Omega)} \\ &\le J(y^*) + \limsup_\gamma (f, y_\gamma)_{L^2(\Omega)} = \frac{1}{2}\|y^*\|^2_{H^1_0(\Omega)},\end{aligned}$$

where we also used the compact embedding of $H^1_0(\Omega)$ into $L^2(\Omega)$. Weak and norm convergence now imply $y_\gamma \to y^*$ in $H^1_0(\Omega)$ as $\gamma \to \infty$. From

$$\|\nabla y_\gamma - p_\gamma\|_{L^2(\Omega)^n} + \|\nabla y^* - \nabla y_\gamma\|_{L^2(\Omega)^n} \ge \|\nabla y^* - p_\gamma\|_{L^2(\Omega)^n}$$

where the left hand side converges to zero for $\gamma \to \infty$, we conclude $p_\gamma \to \nabla y^*$ in $L^2(\Omega)^n$ for $\gamma \to \infty$, which concludes the proof. □

Theorem 1.2 Let $\{(y_\gamma,\, p_\gamma)\}_{\gamma\ge 0}$ in $H^1_0(\Omega) \times L^2(\Omega)^n$ denote the path of solutions of (P^2_γ). Then, $(y_\gamma,\, p_\gamma) \to (y^*,\, \nabla y^*)$ strongly in $H^1_0(\Omega) \times L^2(\Omega)^n$ as $\gamma \to \infty$.

The proof of Theorem 1.2 is similar to the one of Theorem 1.1. Only for proving the boundedness of $\{p_\gamma\}$ we now use the coercivity of J^2_γ with respect to p, and for the feasibility of the limit of the subsequence we use $\big\|(|p_\gamma|_2 - \psi)^+\big\|_{L^2(\Omega)^n} \to 0$ for $\gamma \to \infty$.

Theorem 1.3 Let $\{y_\gamma\}_{\gamma\ge 0}$ in $H^1_0(\Omega)$ denote the path of solutions of (P^3_γ). Then, $y_\gamma \to y^*$ strongly in $H^1_0(\Omega)$ for $\gamma \to \infty$.

Proof. The optimality of y_γ and feasibility of y^* yield

$$\frac{1}{2}\,\|y_\gamma\|^2_{H^1_0(\Omega)} - (f,\, y_\gamma)_{L^2(\Omega)} \le J^3_\gamma(y_\gamma) \le J^3_\gamma(y^*) = J(y^*) \quad \forall\gamma. \tag{1.2}$$

This implies $\|y_\gamma\|_{H^1_0(\Omega)} \le c$ for some constant $c > 0$. Therefore, there exists a subsequence $\{y_{\gamma'}\} \subset \{y_\gamma\}$ such that $y_{\gamma'} \rightharpoonup_{H^1_0} \bar{y}$ as $\gamma' \to \infty$, for some $\bar{y} \in H^1_0(\Omega)$. The weak lower semicontinuity of J and (1.2) yield $J(\bar{y}) \le J(y^*)$. Using (1.2) and the boundedness of $\{y_\gamma\}_\gamma$ we show analogously to the above that

$$\big\|(|\nabla y_\gamma|_2 - \psi)^+\big\|_{L^2(\Omega)^n} \to 0 \text{ for } \gamma \to \infty,$$

which yields feasibility of $\bar{y}$. Finally, by uniqueness of y^* we have $\bar{y} = y^*$. By uniqueness we obtain the weak convergence of the whole sequence $\{y_\gamma\}$. Now similar arguments to those of the proof of Theorem 1.1 yield the strong convergence $y_\gamma \to y^*$ in $H^1_0(\Omega)$ for $\gamma \to \infty$. □

1.3. **First-Order Optimality Conditions.** For solving the optimization problems numerically, we next derive first-order optimality conditions.

Theorem 1.4 For (P^1_γ), there exists $\lambda \in L^2(\Omega)$ with $\lambda(x) \geq 0$ for a.e. $x \in \Omega$ such that

$$(\mathrm{OC}^1_\gamma) \qquad \begin{cases} -(1+\gamma)\Delta y - f + \gamma \operatorname{div} p = 0, \\ -\gamma(\nabla y(x) - p(x)) + \lambda(x) q_p(x) = 0, \\ \lambda(x) \geq 0,\ |p(x)|_2 - \psi(x) \leq 0,\ \lambda(x)(|p(x)|_2 - \psi(x)) = 0 \end{cases}$$

holds with

$$q_p(x) := \begin{cases} \frac{p(x)}{|p(x)|_2} & \text{if } |p(x)|_2 > 0, \\ 0, & \text{else.} \end{cases}$$

Proof. We reformulate (P^1_γ) equivalently as

$$\text{minimize} \quad J^1_\gamma(y,p) + I_{M^1}(p) \quad \text{over } (y,p) \in H^1_0(\Omega) \times L^2(\Omega)^n.$$

The function $J^1_\gamma + I_{M^1}$ is convex on $H^1_0(\Omega) \times L^2(\Omega)^n$ and weakly lower-semicontinuous, thus it is a closed function. Since $(0,0) \in \operatorname{dom}(J^1_\gamma + I_{M^1})$, $J^1_\gamma + I_{M^1}$ is proper. From Prop. 9.5.3 in [3, p.336] we get that (y_γ, p_γ) is an optimal solution of (P^1_γ) iff $0 \in \partial(J^1_\gamma + I_{M^1})(y_\gamma, p_\gamma)$, where ∂ stands for the subdifferential (for convex analysis) with respect to (y_γ, p_γ).

Theorem 1 in [21, p.200] is used for computing $\partial(J^1_\gamma + I_{M^1})(y_\gamma, p_\gamma)$. In fact, since J^1_γ is continuously differentiable, we have $\partial(J^1_\gamma + I_{M^1})(y_\gamma, p_\gamma) = \partial J^1_\gamma(y_\gamma, p_\gamma) + \partial_{p_\gamma} I_{M^1}(p_\gamma)$, where ∂_{p_γ} denotes the subdifferential with respect to p_γ. By Prop. 9.5.4. in [3, p.338], we know that $\partial_{p_\gamma} I_{M^1}(p_\gamma) = N_{M^1}(p_\gamma)$, where the latter object denotes the normal cone to M^1 at p_γ. We define $M^1(x) = \{w \in \mathbb{R}^n \,|\, |w|_2 \leq \psi(x)\}$. By Lemma 6.43 in [5, p.549] we have that

$$N_{M^1}(p_\gamma) = \{\xi \in L^2(\Omega)^n \,|\, \xi(x) \in N_{M^1(x)}(p_\gamma(x)) \text{ a.e. } x \in \Omega\}.$$

Using Prop. 9.6.1. in [3, p.343], we know that for a.e. $x \in \Omega$

$$\begin{aligned} &\xi(x) \in N_{M^1(x)}(p_\gamma(x)) \\ &\Leftrightarrow \exists \lambda(x) \geq 0 : \xi(x) \in \lambda(x) \partial(|\cdot|_2 - \psi)(p_\gamma(x)) \text{ and } \lambda(x)(|p_\gamma(x)|_2 - \psi(x)) = 0. \end{aligned}$$

We know that $\partial(|\cdot|_2 - \psi)(p_\gamma(x)) = Q_{p_\gamma}(x)$ with

$$Q_{p_\gamma}(x) = \begin{cases} \{\frac{p_\gamma(x)}{|p_\gamma(x)|_2}\} & \text{if } |p_\gamma(x)|_2 > 0, \\ \overline{B}(0,1)^n & \text{else,} \end{cases}$$

where $\overline{B}(0,1)^n$ denotes the closed unit ball in $\mathbb{R}^n$ with center 0. Therefore, we have that (y_γ, p_γ) is an optimal solution of (P^1_γ) iff $0 \in \partial(J^1_\gamma + I_{M^1})(y_\gamma, p_\gamma)$ which is equivalent to

$$0 \in \begin{pmatrix} \partial_{y_\gamma} J^1_\gamma(y_\gamma, p_\gamma) \\ \partial_{p_\gamma} J^1_\gamma(y_\gamma, p_\gamma) + N_{M^1}(p_\gamma) \end{pmatrix} \quad \Leftrightarrow \quad 0 \in \begin{pmatrix} \partial_{y_\gamma} J^1_\gamma(y_\gamma, p_\gamma) \\ \partial_{p_\gamma} J^1_\gamma(y_\gamma, p_\gamma) + \xi \end{pmatrix},$$

where $\xi \in L^2(\Omega)^n$ satisfies $\xi(x) \in N_{M^1(x)}(p_\gamma(x))$ a.e. $x \in \Omega$. Therefore, for a.e. $x \in \Omega$ there exists a $\lambda(x) \geq 0$ such that

$$\begin{cases} 0 = -(1+\gamma)\Delta y_\gamma - f + \gamma \operatorname{div} p_\gamma, \\ 0 \in -\gamma(\nabla y_\gamma - p_\gamma)(x) + \lambda(x) Q_{p_\gamma}(x), \\ \text{with } \lambda(x)(|p_\gamma(x)|_2 - \psi(x)) = 0 \text{ for a.e. } x \in \Omega \end{cases}$$

Since for $|p_\gamma(x)|_2 = 0$, we get $\lambda(x) = 0$, we can choose $Q_{p_\gamma}(x) = q_{p_\gamma}(x)$ for a.e. $x \in \Omega$. Since (y_γ, p_γ) is the optimal solution of (P^1_γ), we know that p_γ is feasible. This concludes the proof. □

For (P^2_γ), the associated optimality system reads

$$(\mathrm{OC}^2_\gamma) \qquad \begin{cases} -(1+\gamma)\Delta y - f + \gamma \operatorname{div} p & = 0, \\ -\gamma(\nabla y - p) + \gamma(|p|_2 - \psi)^+ q_p & = 0 \end{cases}$$

with q_p defined as above.

The first order necessary and sufficient optimality condition for (P^3_γ) is given by

$$(\mathrm{OC}^3_\gamma) \qquad -\Delta y - f - \gamma \operatorname{div}\left((|\nabla y|_2 - \psi)^+ Q_{\nabla y}\right) = 0,$$

with $Q_{\nabla y}$ as above and the convention $[(|\nabla y|_2 - \psi)^+ Q_{\nabla y}](x) = 0$ for $|\nabla y(x)|_2 = 0$.

2. Algorithms using Splitting

For the numerical solution of (P^1_γ) we solve the first equation of (OC^1_γ) for fixed $p = p_k \in L^2(\Omega)^n$, and then set $p_{k+1} = P_{M^1}(\nabla y_{k+1})$, where P_{M^1} is the projection onto the set M^1. This is summarized in the following algorithm.

Algorithm 2.1 ((P^1_γ): Algorithm with Projection)

(1) **Initialization.** Choose $p_{\gamma_0} := p_0 \in L^2(\Omega)^n$ and $y_{\gamma_0} := y_0 \in H^1_0(\Omega)$, select $\gamma_0 > 0$, and set $k, \ell := 0$.
   i) **Solve.** Compute $y_{k+1} \in H^1_0(\Omega)$ such that
   $$-(1+\gamma_\ell)\,\Delta y_{k+1} = f - \gamma_\ell \operatorname{div} p_k.$$
   ii) **Project.** $p_{k+1} := P_{M^1}(\nabla y_{k+1})$.
   iii) **Stopping Criterion.** Either stop and set $y_{\gamma_\ell} := y_{k+1}$, $p_{\gamma_\ell} := p_{k+1}$ and go to step (2), or set $k := k+1$ and return to *i*).

(2) **Gamma Update or Stop.** Either stop, or perform a γ-update such that $\gamma_{\ell+1} > \gamma_\ell$, set $\ell := \ell + 1$, and return to *i*).

Lemma 2.2 For p as in step $(1ii)$ of Algorithm 2.1, there exists $\lambda \in L^2(\Omega)$ fulfilling the second equation and the conditions in the third line of (OC^1_γ).

Proof. First we note that the projection P_{M^1} operates pointwise, i.e., if $|\nabla y(x)|_2 \le \psi(x)$, then $p(x) = P_{M^1}(\nabla y)(x) = \nabla y(x)$; otherwise we get $p(x) = P_{M^1}(\nabla y)(x) = [\frac{\nabla y}{|\nabla y|_2}\psi](x)$. In the former case, we set $\lambda(x) := 0$, and in the latter we define $\lambda(x) := \gamma[|\nabla y|_2 - \psi](x)$. One readily shows that with this choice, the second and third lines in (OC^1_γ) are satisfied. □

We next address our choice of stopping rules.

Inner Stopping Criterion; step (1.iii). For fixed $\gamma > 0$, we define

$$\mathrm{res}_1(y,\, p) := -\Delta y - \frac{f}{1+\gamma} + \frac{\gamma}{1+\gamma} \operatorname{div} p \in H^{-1}(\Omega).$$

Then we stop the iteration in step (1) of Algorithm 2.1 as soon as

$$\|\mathrm{res}_1(y_{k+1},\, p_{k+1})\|_{H^{-1}(\Omega)} \le (1 + \left\|\mathrm{res}_1(y_{\gamma_{\ell-1}},\, p_{\gamma_{\ell-1}})\right\|_{H^{-1}(\Omega)})\epsilon_{inner}$$

is fulfilled for some $\epsilon_{inner} > 0$. Here we use $H^{-1}(\Omega) = (H_0^1(\Omega))^*$ and some initial pair $(y_{\gamma_0}, p_{\gamma_0}) \in H_0^1(\Omega) \times L^2(\Omega)^n$.

Outer Stopping Criterion; step (2). Let (y, p, λ) be such that (OC_γ^1) is satisfied. Then from the second equation in (OC_γ^1) we get $\lambda(x)q_p(x) = \gamma(\nabla y(x) - p(x))$ for a.e. $x \in \Omega$. Inserting this into the first equation of (OC_γ^1), we obtain for a.e. $x \in \Omega$

$$-\Delta y - f - \operatorname{div} \lambda q_p = 0 \tag{2.1}$$

$$\lambda(x) \geq 0,\ |p(x)|_2 - \psi(x) \leq 0,\ \lambda(x)(|p(x)|_2 - \psi(x)) = 0 \tag{2.2}$$

Since $\lambda(x) = 0$ for $|p(x)|_2 = 0$, we can select an arbitrary $q_p(x) \in Q_p(x) = \partial_p(|\cdot|_2 - \psi)(p)$. Hence, when $\nabla y = p$, then we have a solution to the original problem. Therefore, for stopping the outer iteration we check whether

$$\|\mathrm{res}_2(y_{\gamma_\ell}, p_{\gamma_\ell})\|_{L^2(\Omega)^n} \leq (1 + \|\mathrm{res}_2(y_{\gamma_0}, p_{\gamma_0})\|_{L^2(\Omega)^n})\epsilon_{outer}.$$

is fulfilled for some fixed $\epsilon_{outer} > 0$, where

$$\mathrm{res}_2(y, p) := \nabla y - p \in L^2(\Omega)^n.$$

In order to solve (P_γ^2) numerically, we consider the second equation in (OC_γ^2). For all $x \in \Omega$ with $|p(x)|_2 \leq \psi(x)$, the equation $-\gamma(\nabla y(x) - p(x)) + \gamma(|p(x)|_2 - \psi(x))^+ q_p(x) = 0$ immediately yields $p(x) = \nabla y(x)$. For all $x \in \Omega$ with $|p(x)|_2 > \psi(x)$ the second equation in (OC_γ^2) leads to

$$\nabla y = p(2 - \frac{\psi}{|p|_2}), \tag{2.3}$$

where we negelect the argument x. Hence there exists $\kappa \in \mathbb{R}$ such that $p = \kappa \nabla y$. Using (2.3) again, we obtain $2\kappa - \frac{\psi}{|\nabla y|_2} = 1$ which yields $\kappa = \frac{1}{2}(1 + \frac{\psi}{|\nabla y|_2})$. These observations lead to the following algorithm.

Algorithm 2.3 ((P_γ^2): Algorithm with Exact p)

(1) **Initialization.** Choose $p_{\gamma_0} := p_0 \in L^2(\Omega)^n$ and $y_{\gamma_0} := y_0 \in H_0^1(\Omega)$, select $\gamma_0 > 0$, and set $k, \ell := 0$.

i) **Solve.** Compute $y_{k+1} \in H_0^1(\Omega)$ such that

$$-(1 + \gamma_\ell)\,\Delta y_{k+1} = f - \gamma_\ell \operatorname{div} p_k,$$

ii) **Set**

$$p_{k+1}(x) = \begin{cases} \nabla y_{k+1}(x) & \text{if } |\nabla y_{k+1}(x)|_2 \leq \psi(x), \\ (\frac{1}{2} + \frac{\psi(x)}{2|\nabla y_{k+1}(x)|_2})\nabla y_{k+1}(x) & \text{else.} \end{cases}$$

iii) **Stopping Criterion.** Either stop and set $y_{\gamma_\ell} := y_{k+1}$, $p_{\gamma_\ell} := p_{k+1}$ and return to step (2), or set $k := k + 1$ and return to *i)*.

(2) **Gamma Update or Stop.** Either stop, or perform γ-update, set $\ell := \ell + 1$, and return to *i)*.

We employ the following stopping rules.

Inner Stopping Criterion. The inner loop is terminated as soon as

$$\|\mathrm{res}_1(y_{k+1}, p_{k+1})\|_{H^{-1}(\Omega)} \leq (1 + \left\|\mathrm{res}_1(y_{\gamma_{\ell-1}}, p_{\gamma_{\ell-1}})\right\|_{H^{-1}(\Omega)})\epsilon_{inner}$$

is fulfilled. As before we use some initial pair $(y_{\gamma_0}, p_{\gamma_0}) \in H_0^1(\Omega) \times L^2(\Omega)^n$.

Outer Stopping Criterion. As before we define $\lambda(x) := 0$ whenever $|\nabla y(x)|_2 \leq \psi(x)$, and $\lambda(x) := \frac{\gamma}{2}(|\nabla y(x)|_2 - \psi(x)) > 0$ otherwise. This motivates the use of

$$\|\mathrm{res}_2(y_{\gamma_\ell}, p_{\gamma_\ell})\|_{L^2(\Omega)^n} \leq (1 + \|\mathrm{res}_2(y_{\gamma_0}, p_{\gamma_0})\|_{L^2(\Omega)^n})\epsilon_{outer}$$

as a stopping rule. In addition, we now also need to check feasibility of p_{k+1}. Thus, we define

$$\mathrm{res}_3(p) = (|p|_2 - \psi)^+ \in L^2(\Omega)$$

and stop the outer iteration as soon as

$$\|\mathrm{res}_3(p_{\gamma_\ell})\|_{L^2(\Omega)} \leq (1 + \|\mathrm{res}_3(p_{\gamma_0})\|_{L^2(\Omega)})\epsilon_{outer}$$

is fulfilled as well.

This concludes our study of the split-penalization methods and we continue with the semismooth Newton method in the next section.

3. A Semismooth Newton Method

3.1. **Newton derivatives and statement of the algorithm.** For every fixed $\gamma > 0$ we propose to solve (OC^3_γ) by a generalized version of Newton's method. For this purpose let $y_{\gamma,k}$ denote the approximation of y^* in iteration k. Since γ is fixed, we write y_k for convenience. Let

$$F_\gamma(y) := -\Delta y - f - \gamma \,\mathrm{div}\left((|\nabla y|_2 - \psi)^+ q_{\nabla y}\right)$$

with q_p and $p = \nabla y$ defined as above on p.6. Since the max-operator is not Fréchet-differentiable, we introduce the notion of Newton-differentiability [14].

Definition 3.1 (Generalized, slant or Newton-derivative) Let X and Z be Banach spaces and let $F\colon D \subset X \to Z$ be a nonlinear mapping with open domain D. Then F is called Newton-differentiable on the open subset $U \subset D$ if there exists a family of generalized derivatives $G\colon U \to \mathcal{L}(X, Z)$ such that

$$\lim_{h\to 0} \frac{1}{\|h\|_X}\|F(x+h) - F(x) - G(x+h)h\|_Z = 0, \quad \text{for every } x \in U.$$

Assume that $q \geq 6$. Using that $\nabla \in \mathcal{L}(W^{1,q}(\Omega), L^q(\Omega)^n)$, $\mathrm{div} \in \mathcal{L}(L^2(\Omega)^n, H^{-1}(\Omega))$, chain rules (see e.g. [27]) and Theorem A.2 in [17, p.1250, s=2] we have that the mapping

$$F_\gamma(\cdot)\colon W^{1,q}_0(\Omega) =: X \to H^{-1}(\Omega)$$

is Newton-differentiable with Newton-map

$$G_{F_\gamma}(y)(\cdot) := -\Delta \cdot -\gamma \,\mathrm{div}\left(L(\nabla y)\nabla \cdot\right) \in \mathcal{L}(X, H^{-1}(\Omega)),$$

where

$$L(p) = G_{max}(|p|_2 - \psi)q_p q_p^T + (|p|_2 - \psi)^+ \frac{1}{|p|_2}(id - q_p q_p^T)$$

with the convention that $[(|p|_2 - \psi)^+ |p|_2^{-1}](x) = 0$ whenever $|p(x)|_2 = 0$. Above, $G_{\max}$ is a Newton derivative of $(\cdot)^+\colon L^q(\Omega)^n \to L^2(\Omega)^n$ (we use the choice in see [16]) and q_p is defined as above on p.6.

We are now ready to specify the algorithm for computing y_γ for a fixed $\gamma > 0$.

Algorithm 3.2 (Semismooth Newton method)

i) **Initialization.** Choose $y_0 \in W_0^{1,q}(\Omega)$, and set $k := 0$.

ii) **Newton Step.** Solve $y_{k+1} \in W_0^{1,q}(\Omega)$

$$\begin{aligned} &- \Delta y_{k+1} - \gamma \operatorname{div}\left(L(\nabla y_k)\nabla y_{k+1}\right) \\ &\qquad = f + \gamma \operatorname{div}\left((|\nabla y_k|_2 - \psi)^+ q_{\nabla y_k}\right) - \gamma \operatorname{div}\left(L(\nabla y_k)\nabla y_k\right) \end{aligned}$$

iii) **Stopping Criterion.** Either stop, or set $k := k + 1$ and return to ***ii)*** .

3.2. **Well-Definedness of the Newton Step.** Existence and uniqueness of $y_{k+1} \in H_0^1(\Omega)$ follows from Lax-Milgram arguments. Next we show that the Newton step yields a unique $y_{k+1} \in W_0^{1,q}(\Omega)$, provided $y_k \in W_0^{1,q}(\Omega)$ for some $q > 2$. For this purpose we use [11, Thm. 1, p.685], where the following definitions are taken from.

Definition 3.3 (R_r) For $2 \le r < \infty$ we denote by R_r the class of all regular subsets G of $\mathbb{R}^n$ for which the duality map J_G maps $W_0^{1,r}(G)$ onto $W^{-1,r}(G)$.

Definition 3.4 (M_p) For $q \ge 2$ we define

$$M_q := \sup\{\|u\|_{W^{1,q}(\Omega)} \mid u \in W_0^{1,q}(\Omega), \|J_\Omega u\|_{W^{-1,q}(\Omega)} \le 1\}.$$

We note that $M_2 = 1$. Setting $k = 0$ and $\kappa = 1$, Definition 2.4. in [32, p.46] of a set Ω having the $N^{k,\kappa}$-property corresponds to Ω having a Lipschitz boundary. From [32, Thm. 2.5, p.55] we know that if Ω has the $N^{0,1}$-property it is $(0,1)$-smooth, which, for bounded sets, corresponds to the definition of regular sets in the sense of Gröger [11, Def.2, p.680]. In Section 5 in [11] it is shown that for every regular Ω there exists $r > 2$ such that $\Omega \in R_r$. The next lemma readily follows from [11, Lemma 1, p.682].

Lemma 3.5 Let $\Omega \in R_r$ for some $r > 2$. Then for all $\epsilon > 0$ there exists some $q \in (2, r]$ such that $M_q \le 1 + \epsilon$.

Lemma 3.6 For $q := 2 + \epsilon$, $n \ge 2$ (in case of $n > 2$, ϵ has to be assumed to be sufficiently small), it holds that

$$W_0^{1,q'}(\Omega) \subset\subset L^2(\Omega) \subset\subset W^{-1,q}(\Omega),$$

where $\frac{1}{q} + \frac{1}{q'} = 1$.

Proof. Use the Rellich-Kondrachov Theorem [1, Thm. 6.3, p.168] and Schauder's Theorem (e.g.[2, p. 387]). □

Theorem 3.7 The solution y_{k+1} computed in step ***ii)*** of Algorithm 3.2 satisfies $y_{k+1} \in W_0^{1,q}(\Omega)$ for some $q > 2$ and for all $k \in \mathbb{N} \cup \{0\}$.

Proof. One readily shows that the bilinear form induced by the terms involving y_{k+1} in the left hand side of the variational equation in ***ii)*** of Algorithm 3.2 is $H_0^1(\Omega)$-coercive with constant 1 and bounded with constant $1 + 3\gamma$. One finds that the associated linear form of the terms on the right hand side is bounded in $H^{-1}(\Omega)$. Hence, the Lax-Milgram Lemma yields the existence of a unique solution in $H_0^1(\Omega)$.

We define $b\colon \Omega \times \mathbb{R}^{n+1} \to \mathbb{R}^{n+1}$ as $b_0(\cdot, \xi) := \xi_0$, $b_j(\cdot, \xi) := \xi_j + \gamma L(\nabla y_k(\cdot))\xi_j$, for $j = 1, \dots, n$. Then, $b(\cdot, 0) = 0 \in L^q(\Omega, \mathbb{R}^{n+1})$, $q > 2$ and $b(\cdot, \xi)$ is measurable for

every $\xi \in \mathbb{R}^{n+1}$. Let $x \in \Omega$ and $\xi, \eta \in \mathbb{R}^{n+1}$, then the coercivity and boundedness conditions on b are fulfilled with $m = 1$ and $M = 1+3\gamma$. Defining $K := (1 - \frac{m^2}{M^2})^{\frac{1}{2}}$, it follows that $K < 1$. From Lemma 3.5 we infer that there exists some $q \in (2, r]$ such that $M_q K < 1$. We further get for all $v \in H_0^1(\Omega)$

$$\int_\Omega b(x,(u,\nabla u)) \cdot (v, \nabla v)\, dx = (u,\, v)_{L^2(\Omega)} + (\nabla u + \gamma L(\nabla y_k)\nabla u,\, \nabla v)_{L^2(\Omega)^n},$$

and we define $R(\cdot) := u(\cdot) + g(\cdot)$, where

$$g = f + \gamma \operatorname{div}\big((|\nabla y_k|_2 - \psi)^+ q_{\nabla y_k}\big) - \gamma \operatorname{div}\big(L(\nabla y_k)\nabla y_k\big).$$

Given $y_k \in W_0^{1,q}(\Omega)$ and using Lemma 3.6, one shows that the right hand side R is an element of $W^{-1,q}(\Omega) = (W_0^{1,q'}(\Omega))^*$. Thus, Theorem 1 in [11, p.685] yields $y_{k+1} \in W_0^{1,q}(\Omega)$, which concludes the proof. □

3.3. **Stopping Criterion.**

Inner Stopping Criterion. We define

$$\mathrm{res}_4(y,\, p) = -\Delta y - f - \gamma \operatorname{div}\big((|\nabla y|_2 - \psi)^+ q_{\nabla y}\big).$$

The inner loop is terminated as soon as

$$\|\mathrm{res}_4(y_{k+1},\, p_{k+1})\|_{H^{-1}(\Omega)} \le (1 + \big\|\mathrm{res}_4(y_{\gamma_{\ell-1}},\, p_{\gamma_{\ell-1}})\big\|_{H^{-1}(\Omega)})\epsilon_{inner}$$

is fulfilled for some constants $\epsilon_{inner} > 0$.

Outer Stopping Criterion. The outer loop is stopped as soon as

$$\|\mathrm{res}_3(\nabla y_{k+1})\|_{L^2(\Omega)^n} \le (1 + \|\mathrm{res}_3(\nabla y_0)\|_{L^2(\Omega)^n})\epsilon_{outer}$$

is fulfilled for some $\epsilon_{outer} > 0$.

3.4. **Convergence Analysis of a Semismooth Newton Method with Lifting.**

While the previous section guarantees for the Newton iterate $y^k \in W_0^{1,\tilde{q}}(\Omega)$ for some $\tilde{q} > 2$, it is known that Newton differentiability of the mapping $F_\gamma : W_0^{1,q}(\Omega) \to H^{-1}(\Omega)$ hinges on $q \ge 6$; compare [17]. Thus, the local convergence analysis of Algorithm 3.2 has to be performed in $W_0^{1,q}(\Omega)$ for $q \ge 6$.

Using Lax-Milgram arguments one can, however, only establish bounded invertibility of the Newton map associated with F_γ as a mapping from $H_0^1(\Omega)$ to $H^{-1}(\Omega)$. Due to the required norm gap for the Newton differentiability of the $\max(0,\cdot)$-operator, however, we would need an appropriate bounded invertibility result for G_{F_γ} defined on $W_0^{1,q}(\Omega)$ for applying the standard semismooth Newton convergence result that guarantees superlinear convergence. Such an invertibility property, however, cannot be expected in general. To establish the local superlinear convergence of the semismooth Newton algorithm here, a lifting step is required. For this purpose assume that there exists an operator satisfying

$$D(\cdot)\colon H_0^1(\Omega) \to W_0^{1,q}(\Omega)$$

such that $\|D(v) - y_\gamma\|_{W_0^{1,q}(\Omega)} \le K_1(\gamma)\,\|v - y_\gamma\|_{H_0^1(\Omega)}$, for some constant $K_1 > 0$. The resulting Newton algorithm can be stated as follows.

Algorithm 3.8 (Semismooth Newton Method with Lifting)

(1) **Initialization.** Choose $y_0 \in W_0^{1,q}(\Omega)$, for $q \ge 6$, select $\gamma_0 > 0$, and let $k, \ell = 0$.

i) **Newton Step.** Solve for $\tilde{y}_{k+1} \in W_0^{1,\tilde{q}}(\Omega)$ such that

$$-\Delta\tilde{y}_{k+1} - \gamma_\ell \operatorname{div}\big(L(\nabla y_k)\nabla\tilde{y}_{k+1}\big) = f + \gamma_\ell \operatorname{div}\big((|\nabla y_k|_2 - \psi)^+ q_{\nabla y_k}\big) - \gamma_\ell \operatorname{div}\big(L(\nabla y_k)\nabla y_k\big).$$

ii) **Lifting Step.** Compute $y_{k+1} = D(\tilde{y}_{k+1})$.

iii) **Stopping Criterion.** Either stop, or set $k := k+1$ and return to ***i)***.

(2) **Gamma Update or Stop.** Either stop, or perform γ-update yielding $\gamma_{\ell+1} > \gamma_\ell$, set $\ell := \ell + 1$ and return to ***i)***.

The next theorem ensures local superlinear convergence of the semismooth Newton scheme stated in Algorithm 3.8.

Theorem 3.9 Let $\gamma > 0$ be fixed and suppose that $y_\gamma \in W_0^{1,q}(\Omega)$ satisfies $F_\gamma(y_\gamma) = 0$. Moreover, for given $y_k \in W_0^{1,q}(\Omega)$, define $\tilde{y}_{k+1}$ as the solution of step ***i)*** in Algorithm 3.8 and $y_{k+1} \in W_0^{1,q}(\Omega)$ as the solution of the lifting step ***ii)*** in Algorithm 3.8. Then the sequence $\{y_k\} \subset W_0^{1,q}(\Omega)$ generated by the Newton-iteration with lifting step converges superlinearly to y_γ, provided $y_0 \in W_0^{1,q}(\Omega)$ is sufficiently close to y_γ.

Proof. By assumption we have that $y_0 \in B_0^{1,q}(y_\gamma;\rho) := \{z \in W_0^{1,q}(\Omega) : \|z - y_\gamma\|_{W_0^{1,q}(\Omega)} < \rho\}$ for some $\rho > 0$. From the Newton step and by the Lax-Milgram Lemma, we have that

$$\begin{aligned}&\|\tilde{y}_{k+1} - y_\gamma\|_{H_0^1(\Omega)}\\ &\le \big\|G_{F_\gamma}(y_k)^{-1}\big\|_{\mathcal{L}(H^{-1},\,H_0^1,\,\Omega)} \big\|F_\gamma(y_k) - F_\gamma(y_\gamma) - G_{F_\gamma}(y_k)(y_k - y_\gamma)\big\|_{H^{-1}(\Omega)}\end{aligned} \tag{3.1}$$

and further $\big\|G_{F_\gamma}(y_k)^{-1}\big\|_{\mathcal{L}(H^{-1},\,H_0^1,\,\Omega)} \le c$ for some $c > 0$ independent of k, but depending on γ. Since F_γ is Newton-differentiable on $W_0^{1,q}(\Omega)$ with Newton derivative G_{F_γ} and $y_k \in W_0^{1,q}(\Omega)$, for some constant $K_2 > 0$ it follows that

$$\|\tilde{y}_{k+1} - y_\gamma\|_{H_0^1(\Omega)} \le K_2 \|y_k - y_\gamma\|_{W_0^{1,q}(\Omega)}, \tag{3.2}$$

upon possibly reducing $\rho > 0$. Using the definition of y_{k+1} and $\tilde{y}_{k+1} \in W_0^{1,\tilde{q}}(\Omega) \subset H_0^1(\Omega)$, we get

$$\|y_{k+1} - y_\gamma\|_{W_0^{1,q}(\Omega)} \le K_1 \|\tilde{y}_{k+1} - y_\gamma\|_{H_0^1(\Omega)},$$

for some constant $K_1 > 0$. Thus, choosing $K_2 < \frac{1}{K_1}$ we have

$$\frac{\|y_{k+1} - y_\gamma\|_{W_0^{1,q}(\Omega)}}{\|y_k - y_\gamma\|_{W_0^{1,q}(\Omega)}} \overset{(3.2)}{\le} \frac{K_2 K_1 \|y_k - y_\gamma\|_{W_0^{1,q}(\Omega)}}{\|y_k - y_\gamma\|_{W_0^{1,q}(\Omega)}} < 1.$$

It follows that $y_k \to y_\gamma$ for $k \to \infty$ in $W_0^{1,q}(\Omega)$ and it further holds that

$$\frac{\|y_{k+1} - y_\gamma\|_{W_0^{1,q}(\Omega)}}{\|y_k - y_\gamma\|_{W_0^{1,q}(\Omega)}} \le \frac{K_1 \|\tilde{y}_{k+1} - y_\gamma\|_{H_0^1(\Omega)}}{\|y_k - y_\gamma\|_{W_0^{1,q}(\Omega)}} \overset{(3.1)}{\le} \frac{\mathcal{O}\left(\|y_k - y_\gamma\|_{W_0^{1,q}(\Omega)}\right)}{\|y_k - y_\gamma\|_{W_0^{1,q}(\Omega)}} \to 0,$$

for $k \to \infty$, where $\mathcal{O}(t)/t \to 0$ for $t \to 0$ with $\mathcal{O}(\cdot)$ depending on our fixed choice of γ. This concludes the proof. □

Concerning the explicit form of the lifting operator we remark that it can be computed in special cases as shown, for instance, in [14]. In our context, however,

finding such a smoothing operator D seems to be difficult. Moreover, numerically the algorithm does not seem to need the extra smoothing, as it works in a stable way and exhibits (mesh independent) superlinear convergence without lifting (cf. Section 5).

4. Path-Following Methods

In this chapter we develop exact and inexact path-following methods for updating γ. For this purpose we utilize a model function m, which mimics the behavior of the so-called path value functional. In addition, the inexact path-following method uses feasibility and complementarity measures to update γ. The γ-update is done in the *outer* algorithm, once the *inner iteration*, i.e., solving for y_γ for fixed γ, terminates successfully.

4.1. The Path Value Functional.

Our automatic adaptive updating strategy for the path parameter γ relies on the path value functional, which we study next.

Definition 4.1 (Path Value Functional) The functional

$$\gamma \mapsto V(\gamma) := J^i_\gamma(y_\gamma, p_\gamma),$$

for $i \in \{1, 2\}$ respectively

$$\gamma \mapsto V(\gamma) := J^3_\gamma(y_\gamma),$$

defined on $(0, \infty)$ is called the *path value functional* associated to J^j_γ for $j \in \{1, 2, 3\}$.

The functional $V(\cdot)$ immediately inherits the boundedness from the respective properties of the path $\{y_\gamma, p_\gamma\}_\gamma$ respectively $\{y_\gamma\}_\gamma$. In addition it turns out that V enjoys differentiability properties. As our subsequent γ-update strategy monotonically increases γ, the specific directional differentiability would be sufficient for our purposes. Here, however, we prove more: First we establish local Lipschitz continuity of y_γ with respect to γ and then differentiability of the value functional.

Proposition 4.2 The solution y_γ of (P^3_γ) is locally Lipschitz continuous in γ, i.e., for $\gamma > 0$ there exists a constant $C(\gamma) > 0$ depending on γ such that

$$\|y_{\gamma'} - y_\gamma\|_{H^1_0(\Omega)} \leq C(\gamma)|\gamma' - \gamma|$$

for $\gamma' > 0$.

Proof. Let $\mathfrak{p}(y) := \frac{1}{2}\|(|\nabla y|_2 - \psi)^+\|^2_{L^2(\Omega)}$. Then the first-order optimality condition for (P^3_γ) is equivalent to

$$\frac{1}{\gamma}(\Delta y_\gamma + f) \in \partial \mathfrak{p}(y_\gamma)$$

or, by utilizing the subgradient inequality (not however that $\mathfrak{p}$ is continuously differentiable),

$$\langle \frac{1}{\gamma}(\Delta y_\gamma + f), y - y_\gamma \rangle + \mathfrak{p}(y_\gamma) \leq \mathfrak{p}(y) \quad \forall y \in H^1_0(\Omega), \tag{4.1}$$

where $\langle\cdot,\cdot\rangle$ denotes the duality pairing between $H^{-1}(\Omega)$ and $H_0^1(\Omega)$. Considering (4.1) for (γ, y_γ) and $(\gamma', y_{\gamma'})$ with $\gamma' > 0$, and $y = y_{\gamma'}$ in the former and $y = y_\gamma$ in the latter case, respectively, then adding the resulting inequalities yields

$$\langle \frac{1}{\gamma}(\Delta y_\gamma + f) - \frac{1}{\gamma'}(\Delta y_{\gamma'} + f), y_{\gamma'} - y_\gamma \rangle \leq 0.$$

From adding and subtracting $\frac{1}{\gamma'}\Delta y_\gamma$ and estimating we infer

$$\frac{1}{\gamma'}\|y_{\gamma'} - y_\gamma\|^2_{H_0^1(\Omega)} \leq \big|\frac{1}{\gamma} - \frac{1}{\gamma'}\big| \, \|f + \Delta y_\gamma\|_{H^{-1}(\Omega)} \|y_{\gamma'} - y_\gamma\|_{H_0^1(\Omega)}.$$

Thus, we have

$$\|y_{\gamma'} - y_\gamma\|_{H_0^1(\Omega)} \leq \frac{|\gamma' - \gamma|}{\gamma} \|f + \Delta y_\gamma\|_{H^{-1}(\Omega)}.$$

From the proof of Theorem 1.3 we know that $\{y_\gamma\}$ is uniformly bounded (w.r.t γ) in $H_0^1(\Omega)$. This fact and the above estimate yield the existence of a constant $C(\gamma) > 0$ depending on γ such that

$$\|y_{\gamma'} - y_\gamma\|_{H_0^1(\Omega)} \leq C(\gamma)|\gamma' - \gamma|$$

as was to be shown. □

Theorem 4.3 For every $\gamma > 0$, the path value function $V(\gamma) = J^3_\gamma(y_\gamma)$ is continuously differentiable with

$$V'(\gamma) = \frac{1}{2} \left\| (|\nabla y_\gamma|_2 - \psi)^+ \right\|^2_{L^2(\Omega)}.$$

Proof. Let $\delta_\gamma \in \mathbb{R}$ be arbitrary, but fixed. From the definition of $V(\gamma)$ we obtain for $t > 0$

$$\frac{V(\gamma + t\delta_\gamma) - V(\gamma)}{t} \geq \frac{\delta_\gamma}{2} \|(|\nabla y_{\gamma + t\delta_\gamma}| - \psi)^+\|^2_{L^2(\Omega)}. \tag{4.2}$$

On the other hand, we obtain

$$\begin{aligned} \frac{V(\gamma + t\delta_\gamma) - V(\gamma)}{t} &\leq \frac{1}{t}\Big(J(y_\gamma) + \frac{\gamma + t\delta_\gamma}{2} \|(|\nabla y_\gamma| - \psi)^+\|^2_{L^2(\Omega)} \\ &\qquad - J(y_\gamma) - \frac{\gamma}{2}\|(|\nabla y_\gamma| - \psi)^+\|^2_{L^2(\Omega)} \Big) \\ &= \frac{\delta_\gamma}{2} \|(|\nabla y_\gamma| - \psi)^+\|^2_{L^2(\Omega)} \end{aligned} \tag{4.3}$$

Combining (4.2) and (4.3) and applying Proposition 4.2 yields

$$\begin{aligned} \frac{\delta_\gamma}{2}\|(|\nabla y_\gamma| - \psi)^+\|^2_{L^2(\Omega)} &\leq \liminf_{t \downarrow 0} \frac{V(\gamma + t\delta_\gamma) - V(\gamma)}{t} \\ &\leq \limsup_{t \downarrow 0} \frac{V(\gamma + t\delta_\gamma) - V(\gamma)}{t} \leq \frac{\delta_\gamma}{2}\|(|\nabla y_\gamma| - \psi)^+\|^2_{L^2(\Omega)}. \end{aligned}$$

Observing that $V'(\gamma; \delta_\gamma)$ is bounded and linear in δ_γ along with continuity with respect to γ proves the assertion. □

Analogously to Theorem 4.3, one proves the following results.

Theorem 4.4 For every $\gamma > 0$, the path value function $V(\gamma) = J^1_\gamma(y_\gamma)$ is continuously differentiable with

$$V'(\gamma) = \frac{1}{2} \|\nabla y_\gamma - p_\gamma\|^2_{L^2(\Omega)^n}.$$

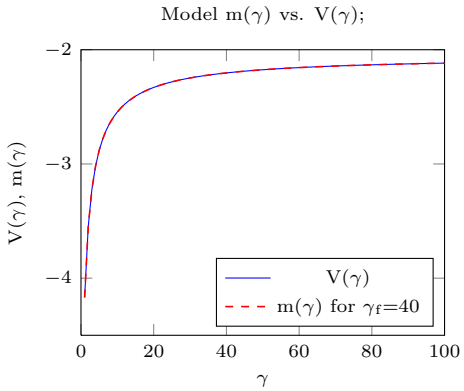

Figure 1. Graph of $V(\gamma)$ and m_{γ_ℓ} for $\gamma_\ell = 40$, for testproblem P2 with mesh size $h = 1/128$, step size of γ is 1 for (P^3_γ), i.e. solved with semismooth Newton.

Theorem 4.5 For every $\gamma > 0$, the path value function $V(\gamma) = J^2_\gamma(y_\gamma)$ is continuously differentiable with

$$V'(\gamma) = \frac{1}{2}\left\|\nabla y_\gamma - p_\gamma\right\|^2_{L^2(\Omega)^n} + \frac{1}{2}\left\|(|p_\gamma|_2 - \psi)^+\right\|^2_{L^2(\Omega)}.$$

In the following, we refer to $V'(\cdot;\cdot)$ simply as V'.

4.2. **Model Function.** Assume that some γ-value $\gamma_\ell > 0$, $\ell \in \mathbb{N}$, is given such that y_{γ_ℓ} is not stationary for the original problem. Our ansatz for a model function m_ℓ approximating the value functional V along the path with $m_\ell(\gamma_\ell) = V(\gamma_\ell)$ is motivated by the facts, that V satisfies $V'(\gamma) > 0$ as well as $\lim_{\gamma\to\infty} V(\gamma) = J(y^*)$. Thus, we consider functions of the form

$$m_\ell(\gamma) = C_{1,\ell} - \frac{C_{2,\ell}}{E_\ell + \gamma} \tag{4.4}$$

with $C_{1,\ell} \in \mathbb{R}$, $C_{2,\ell} \geq 0$, $E_\ell > 0$. The parameters are determined by invoking the conditions $m_\ell(0) = V(0)$, $m_\ell(\gamma_\ell) = V(\gamma_\ell)$, $m'_\ell(\gamma_\ell) = V'(\gamma_\ell)$:

$$\begin{aligned} E_\ell &= \gamma_\ell^2 V'(\gamma_\ell)\big(V(\gamma_\ell) - V(0) - \gamma_\ell V'(\gamma_\ell)\big)^{-1}, \\ C_{2,\ell} &= \gamma_\ell^{-1} E_\ell(E_\ell + \gamma_\ell)\big(V(\gamma_\ell) - V(0)\big), \\ C_{1,\ell} &= V(0) + \frac{C_{2,\ell}}{E_\ell}, \end{aligned}$$

for a given reference point $\gamma_\ell > 0$. We note that for $\gamma = 0$, $m_\ell(0) = V(0) = J(y^\circ)$ holds true, where y° minimizes J over $H^1_0(\Omega)$. Given γ_ℓ, the model function is then used to determine a suitable $\gamma_{\ell+1} > \gamma_\ell$. In Figure 1 we compare the model function m and the value functional V for $\gamma_\ell = 40$ in case of (P^3_γ), i.e., solved with our semismooth Newton method, over the interval $(0, 100)$. We clearly observe an excellent fit of the model function in this case.

4.3. **Exact Path-Following.** As argued before, we have $V'(\gamma) \geq 0$ in $(0, \infty)$, $V(0) = J(y^\circ)$ and $\lim_{\gamma\to\infty} V(\gamma) = J(y^*) =: V^*$. Thus, we may assume that the tangent to V at a certain point $\gamma_\ell > 0$, i.e.,

$$t_\ell(\gamma) := V(\gamma_\ell) + V'(\gamma_\ell)(\gamma - \gamma_\ell),$$

evaluated at $\gamma = 0$ is larger than $V(0)$, i.e. $t_\ell(0) > V(0)$. Hence, it follows that $V(\gamma_\ell) - V'(\gamma_\ell)\gamma_\ell > V(0)$ for every $\gamma_\ell > 0$, and we have $E_\ell, C_\ell > 0$ for all $\gamma_\ell \in (0, \infty)$. This implies that $m_\ell(\gamma) \leq C_{1,\ell}$ and $m_\ell(\gamma) \to C_{1,\ell}$ for $\gamma \to \infty$.

As a consequence, we propose the following update strategy for γ: Let τ_ℓ satisfy $\tau_\ell \in (0,1)$ for all $\ell \in \mathbb{N}$ and $\tau_\ell \downarrow 0$ as $\ell \to \infty$ and assume that $V(\gamma_\ell)$ is available. Then, given γ_ℓ the updated value $\gamma_{\ell+1}$ should ideally satisfy

$$|V^* - V(\gamma_{\ell+1})| \leq \tau_\ell |V^* - V(\gamma_\ell)|. \tag{4.5}$$

Since $V(\gamma_{\ell+1})$ and V^* are unknown, we use our model $m_\ell(\gamma)$ at $\gamma = \gamma_{\ell+1}$ and for $\gamma \to \infty$ in order to estimate these two quantities. Thus, (4.5) is replaced by

$$|C_{1,\ell} - m_\ell(\gamma_{\ell+1})| \leq \tau_\ell |C_{1,\ell} - V(\gamma_\ell)| =: \beta_\ell. \tag{4.6}$$

Utilizing the structure of m_ℓ and assuming equality in (4.6) we obtain

$$\gamma_{\ell+1} = \frac{C_{2,\ell}}{\beta_\ell} - E_\ell. \tag{4.7}$$

It remains to prove that $\gamma_{\ell+1} > \gamma_\ell$. Since $m_\ell(\gamma) \leq C_{1,\ell}$ and by definition of $m_\ell(\gamma_\ell)$ we have that $V(\gamma_\ell) = m_\ell(\gamma_\ell)$. Together with the facts that $\tau_\ell \in (0,1)$, $C_{2,\ell} > 0$, and $E_\ell > 0$ this leads to

$$\frac{C_{2,\ell}}{E_\ell + \gamma_{\ell+1}} \leq \tau_\ell \Big(\frac{C_{2,\ell}}{E_\ell + \gamma_\ell} \Big) < \frac{C_{2,\ell}}{E_\ell + \gamma_\ell}.$$

Thus, $\gamma_{\ell+1} > \gamma_\ell$ for all $\ell = 0, 1, \ldots$ (compare [15, p.177]).

Utilizing the γ-update based on (4.5) may result in a rapid γ-increase. This may adversely effect the condition number of the linear systems in the inner loop early along the outer iterations. In order to keep the algorithm stable in this respect, we safeguard the γ-update by prohibiting large deviations of the tangent from the model. Indeed, if necessary, then we reduce the actual γ-value until

$$|t_\ell(\gamma_{\ell+1}) - m_\ell(\gamma_{\ell+1})| \leq \tau_1 |V(\gamma_\ell) - V(\gamma_{\ell-1})| \tag{4.8}$$

with $\tau_1 \in (0,1)$, $t_\ell(\gamma) = V(\gamma_\ell) + V'(\gamma_\ell)(\gamma - \gamma_\ell)$ and $m_\ell(\gamma)$ the model related to γ_ℓ. Numerically, $V(\gamma)$ is approximated by computing $J^i_\gamma(y_{k+1}, p_{k+1})$ $i \in \{1,2\}$ respectively $J^3_\gamma(y_{k+1})$. This safeguard strategy is motivated by the good approximation quality of our model as indicated by Figure 1. Note that for small γ the distance between t_ℓ and m_ℓ might be large, but so we expect $|V(\gamma_\ell) - V(\gamma_{\ell-1})|$ as the change in the function value is supposed to be rather large for small γ. However, for large γ both difference measures tend to be small. Since this strategy requires information at $\gamma_{\ell-1}$, we only use it once at least three γ-updates have been performed. In case $\gamma_{\ell+1} \gg \gamma_\ell$ for $\ell = 1, 2$, we use a rather conservative γ-update, i.e. $\gamma_{\ell+1} = \gamma_\ell + c$, for some constant $c > 0$. With this update strategy in mind, we implemented the following algorithm:

Algorithm 4.6 (Outer Algorithm)

- ***i*) Initialization.** Select $\gamma_0 > 0$; set $\ell := 0$.
- ***ii*) Inner Algorithm.** Apply Algorithm 3.2 to obtain y_{k+1,γ_ℓ}.
- ***iii*) Gamma-Update.** If $\ell < 3$ apply the conservative update as described above; otherwise compute $V(\gamma_\ell)$, $V'(\gamma_{\ell+1})$ and $\gamma_{\ell+1}$ according to (4.7), and if $\gamma_{\ell+1} >> \gamma_\ell$, reduce $\gamma_{\ell+1}$ until (4.8) is satisfied.
- ***iv*) Stopping Criterion.** Either stop, or set $\ell := \ell + 1$, and go to ***ii*)**.

The same strategy can be used for Algorithm 2.1 and 2.3. We note that below we occasionally use the short hand notation $y_{k+1,\gamma_\ell} = y_{\gamma_\ell}$ for the (approximate solution) when referring to the inner/outer stopping rules.

4.4. **Inexact Path-Following.** While exact path-following relies on the fact that for every γ_ℓ the corresponding point on the path is computed, this is not the case for inexact techniques. For inexact path-following the iterates must only stay within the neighborhood of the path. Therefore a different update strategy for the path parameter γ is required. Such a strategy aims to keep the number of iterations as small as possible while still maintaining (fast) convergence of the method. For that reason inexact path-following methods are usually more relevant in practice than exact ones.

We denote $z = (y, p) \in H_0^1(\Omega) \times L^2(\Omega)^n$ in case of problems (P_γ^1) and (P_γ^2) and $z = y \in H_0^1(\Omega)$ in case of (P_γ^3). We start by defining the neighborhood

$$N(\gamma) := \big\{ z \,\big|\, \|\mathrm{res}(z)\|_{H^{-1}(\Omega)} \le \frac{\tau_2}{\gamma} \big\} \tag{4.9}$$

where $\tau_2 > 0$ denotes some fixed parameter and res is the associated inner residuum dependent on the corresponding z. Then we terminate the inner loop as soon as it reaches $N(\gamma)$. Hence, we compute increasingly more accurate solutions to (OC_γ^j) for $j \in \{1, 2, 3\}$ as γ increases and we allow significant violations early along the γ-updates. Thus, in contrast to exact path-following we should never expect to have $V(\gamma)$ available for finite $\gamma > 0$. Consequently, when computing the model m, we replace $V(\gamma)$ by $J_\gamma^j(z_{k+1,\gamma})$ for $j \in \{1, 2, 3\}$, where $z_{k+1,\gamma}$ denotes the first iterate of the inner iteration satisfying $z_{k+1,\gamma} \in N(\gamma)$.

In order to safeguard large deviations $|V(\gamma) - J_\gamma^j(z_{k+1,\gamma})|$, $j \in \{1, 2, 3\}$, we propose the following γ-update strategy:

For arbitrary $y \in H_0^1(\Omega)$ we define

$$\mathcal{P}_{k+1}^\gamma := \{x \in \Omega \,|\, |\nabla y_{k,\gamma}|_2 - \psi > 0\}, \quad \mathcal{N}_{k+1}^\gamma := \Omega \setminus \{\mathcal{P}_{k+1}^\gamma\}.$$

If it is clear in the context, we leave off the arguments "∇y". Let $\rho_\cdot^F$ denote the primal infeasibility measure

$$\rho_{k+1}^F \quad := \quad \int_\Omega (|\nabla y_{k+1,\gamma}|_2 - \psi)^+ \, dx$$

and $\rho_\cdot^C$ represent the complementarity measures

$$\rho_{k+1}^C \quad := \quad \int_{\mathcal{N}_{k+1}^\gamma} (|\nabla y_{k+1,\gamma}|_2 - \psi)^+ \, dx + \int_{\mathcal{P}_{k+1}^\gamma} (|\nabla y_{k+1,\gamma}|_2 - \psi)^- \, dx,$$

where $(\cdot)^- = -\min(0, \cdot)$. If $\mathcal{P}_{k+2}^\gamma = \mathcal{P}_{k+1}^\gamma$ and $\mathcal{N}_{k+2}^\gamma = \mathcal{N}_{k+1}^\gamma$, then the complementarity measure ρ_{k+1}^C vanishes, assuming sufficiently accurate solutions of the linear systems in our Newton iteration. The feasibility measure $\rho_\cdot^F$ vanishes when y_{k+1} is feasible on Ω. Note that $\rho_{k+1}^F > \rho_{k+1}^C$ in the infeasible case.

Based on these observations we propose the following criterion for updating γ. A similar update strategy can be found in [15].

$$\gamma_{k+1} \ge \max\Big(\gamma_k \max\big(\tau_3, \frac{\rho_{k+1}^F}{\rho_{k+1}^C}\big), \ \frac{1}{(\rho_{k+1}^F)^\kappa}\Big), \tag{4.10}$$

with $\tau_3 > 0$ and $\kappa \ge 1$. The first term in the outermost max-expression is used to determine the impact of the various measures in the following sense: If, in $\frac{\rho_\cdot^F}{\rho_\cdot^C}$,

$\rho_\cdot^C$ is small compared to $\rho_\cdot^F$, we find that the iterates primarily lack feasibility as compared to complementarity. Thus, we need a large γ-update which aims at reducing constraint infeasibility. We note that $\rho_\cdot^F \gg \rho_\cdot^C$ might also be a consequence of our inexact solves. Increasing γ and requiring $y_{k,\gamma} \in N(\gamma)$ enforce a reduction in feasibility violation; alternatively one may reduce τ_2 for the current given γ-value and monitor the progress of the feasibility violation. Only if the latter does not reduce sufficiently relative to $\rho_\cdot^C$, then a γ-update is performed. The latter option, however, was not implemented in our algorithm. If the fraction is close to 1 though, i.e. the measures are about the same size, we cannot come to any conclusions by evaluating them. Then, $\tau_3 > 1$ will dominate this inner max-expression. In case that the measures are all rather small, then the second term in the outer max-expression should yield a significant increase in γ. Here the power $\kappa \geq 1$ induces growth rates for $\{\gamma_k\}$.To prevent the update γ_{k+1} based on (4.10) from becoming too large when compared to γ_k, we safeguard the γ-updates by using model functions $m(\gamma)$, as we did in Subsection 4.3 in the exact case (cf. (4.8), p.16). If some of the constraints are inactive, the feasibility measures may get zero. Also, it may happen that the complementarity measures are equal to zero at some point, if the active sets of two successive iterates are the same, even though they are not quite feasible enough. Numerically, we have to take precautions for that case.

5. Numerical Test Runs

For the implementation $\Omega = (0,1)^2$ was chosen and uniformly discretized via the Finite-Element-Method. For discretizing $H_0^1(\Omega)$ we use globally continuous P^1-elements and p is approximated by piecewise constant functions on the triangles of the underlying triangulation of Ω. By h we denote the underlying mesh size. In all cases, the starting point y_0 was chosen as the unconstrained minimizer y° of (P). Our stopping rules involve the H^{-1}-norm of (parts of) the residual r, i.e. $\|r\|_{H^{-1}(\Omega)}$. Numerically, we realize this norm by solving $-\Delta R = r$ in $H^{-1}(\Omega)$ for $R \in H_0^1(\Omega)$ and taking $\|\nabla R\|_{H_0^1(\Omega)}$. We also note that the linear systems occurring in our algorithms are solved by sparse direct solvers in MATLAB.

For path following, the parameters were set as $\tau_1 = 0.1$, $\tau_2 = 1$, $\tau_3 = 2$, $\kappa = 5$. (cf. p.17 et seq.). For exact path-following, to ensure $\tau_\ell \in (0,1)$, if $\tau_\ell > 1$ we first set it to 0.5 and then use $\tau_\ell = \frac{\tau_{\ell-1}}{2}$ as a safeguard while ℓ is still small. We note that the choices of τ_i, $i = 1,2,3$, are not critical; for κ we found a range of $[2,5]$ useful. Larger κ-values usually lead to large γ-updates by (4.13) towards the end of the iterations. In the latter case, the tangent condition, however, usually reduced too aggressive choices of γ.

The subsequent discussion is based on the following test problems.

Test problem P1. This test problem is chosen for validation purposes. In fact, when f and ψ are constant, then the gradient constrained problem can be reformulated as an obstacle type problem of the form

$$(\mathrm{P}_{obstacle}) \qquad \begin{aligned} &\text{minimize } \frac{1}{2}\|y\|_{H_0^1(\Omega)} - (f,\, y)_{L^2(\Omega)} \quad \text{over } y \in H_0^1(\Omega) \\ &\text{s.t } |y(x)| \leq \Psi_d(x) \text{ a.e. in } \Omega, \end{aligned}$$

for $\Psi_d(x) := \min_{z\in\partial\Omega} |z - x|_2$; ; see, e.g., [6, 10]. Thus, we may compare our solvers with a rather standard semismooth Newton solver like the one stated in [14] and validate the obtained solutions.

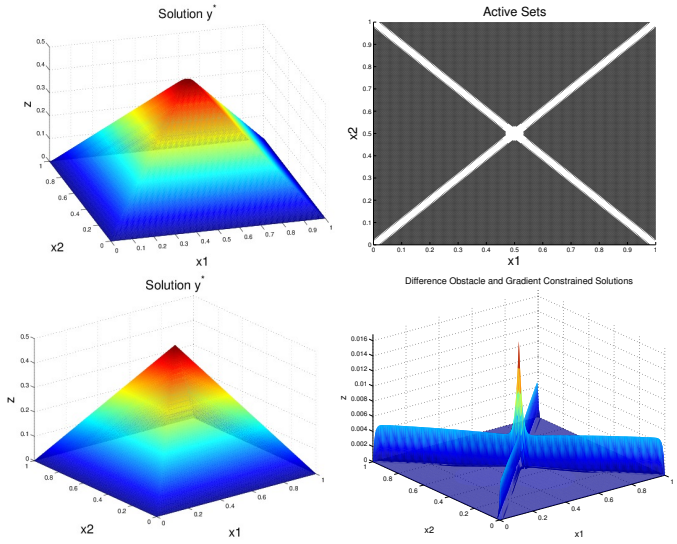

Figure 2. Optimal solution y^* for test problem P1 (upper left plot), the active sets (upper right plot, active sets plotted in black), solution plot solved by an Obstacle Problem solver (lower left plot) and difference of the solution plots (lower right plot), everything for test problem P1 for (P^3_γ), i.e., using the semismooth Newton method, mesh size $h = \frac{1}{256}$.

In our tests we choose $f \equiv 50$ and $\psi \equiv 1$. The solution plot of the obstacle problem is found in the lower left plot of Figure 2. On the lower left of Figure 2 the absolute value of the difference of the solution of the gradient constrained and the obstacle problem is plotted. Here, we show the solution plot of (P^3_γ) but the other methods yield very similar solution plots. As one can see in the plots, the edges of the solution of the obstacle problem are sharper than the gradient constrained one. This correlates to the plot of the active sets where one can see that the constraint is not active on the edges. Accordingly the difference plot shows that the deviations of the solutions lie mostly on the edges and on the peak of the pyramid. This behavior can be attributed to the numerical approximation of the gradient operator contained in the constraint set. In summary, we see that our gradient constrained method solves the problem satisfactorily. In Figure 3 we show for our method using projected p the corresponding constrained gradients and the associated p in case of test problem P1 . Clearly, one can see in Figure 3, that the gradients were constrained to $\psi = 1$ and p approximates the gradient of the solution very well.

Test problem P2. In this test problem we choose a non-constant right hand side, i.e., the reformulation of the gradient constrained problem as an obstacle problem is no longer available. Moreover, our choice of data yields a non-symmetric active set with respect to the vertical axis as can be observed in Figure 4.

In fact, we consider $\psi \equiv 1$ and

$$f(x) = \begin{cases} 0 & \text{if } 0 \le x_1 \le 0.5, \\ 3200 - 19200x_1 + 41600x_1^2 - 38400x_1^3 + 12800x_1^4 & \text{if } 0.5 < x_1 \le 1. \end{cases}$$

The solution y^*, the corresponding active sets at the solution and the right hand side f are shown in the plots in Figure 4. As one can see in the active set plot, the constraint is only active on the right hand side of the coordinate plane with

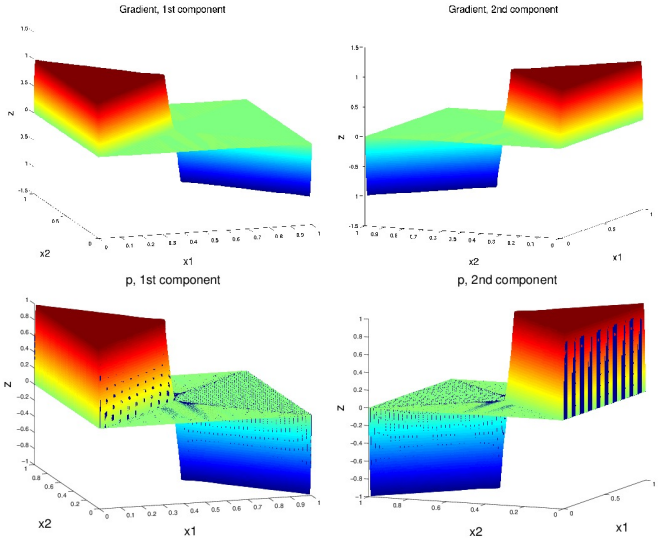

Figure 3. The first component of the gradient (upper left plot), the second component of the gradient (upper right plot) for test problem P1 , Parameter p (lower plots) for test problem P1 using (P^1_γ), i.e., p calculated via projection, mesh size $h = \frac{1}{256}$.

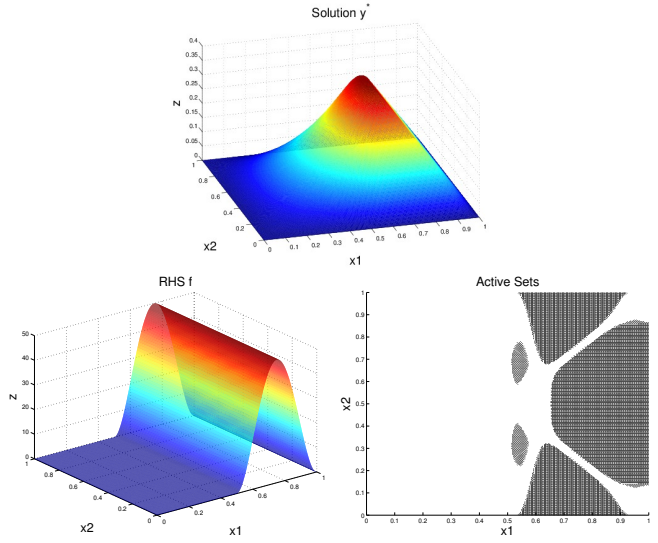

Figure 4. Optimal solution y^* (upper plot), right hand side f (lower left plot) and the active sets (lower right plot, active sets plotted in black) for test problem P2 using (P^1_γ), i.e., p calculated via projection, mesh size $h = \frac{1}{256}$.

respect to x_1 which corresponds to the right hand side f. Accordingly, the solution is constrained only in this region. As one can see in Figure 5 the gradients were constrained to $\psi = 1$. In regions where the constraints are active, we observe a plateau at 1 in the gradient plots. We find that p approximates the gradient of the solution very well.

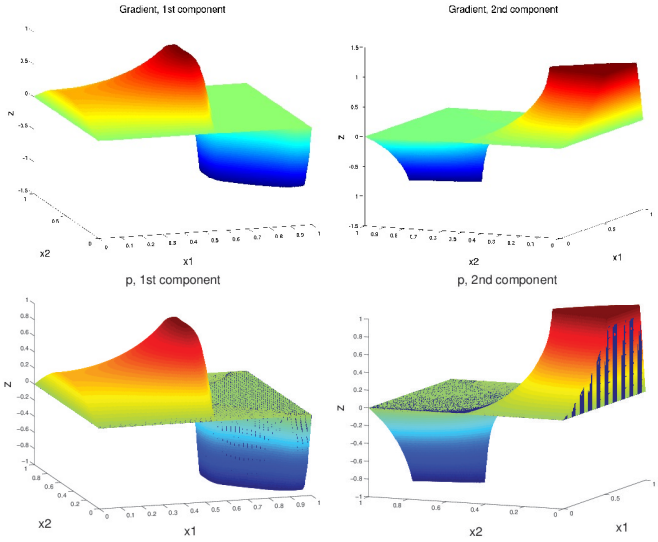

Figure 5. The first component of the gradient (upper left plot), the second component of the gradient (upper right plot), Parameter p (lower plots) for test problem P2 using (P_γ^1), i.e., p calculated via projection, mesh size $h = \frac{1}{256}$.

Test problem P3. In order to further demonstrate the possible practical impact of the numerical methods studied in this paper, we consider a problem that arises in the area of superconductivity. The original problem formulation leads to a quasi-variational inequality with an upper bound ψ depending on y, i.e., $\psi = \Psi(y)$; see [24]. A possible solution scheme for the quasi-variational inequality problem consist in lagging the y-dependent bound behind, i.e., given some approximation y^i one computes y^{i+1} by solving (P) with $\psi = \Psi(y^i)$. Thus, the resulting subproblems then fall into the framework considered in this paper.

We take the example in Section 3 in [24] for $p = 2$ and $u = g$ on $\partial\Omega$. For obtaining a system with nonzero right hand side f and homogeneous Dirichlet boundary conditions, as studied in this work, we extend g to g_{ext} such that $g_{ext|\partial\Omega} = g$, reformulate the system in [24] and solve (P). In our tests we choose g_{ext} such that $\Delta g_{ext}(x) =: f(x) = 800x_1^2 - 1600x_1^3 + 800x_1^4$. The upper bound $\Psi(y)$ is chosen according to Kim's model as described in [4]. In fact setting $y = y^\circ$, the solution of the unconstrained problem, we use $\Psi(y^\circ) = (1 + \frac{|y^\circ|_2}{a})^{-1}$, where $a = 0.02$. Numerically, to approximate ψ as a piecewise constant function on the elements we used the largest values at the three nodes associated to the triangle. The solution y^*, the constraint ψ, right hand side f and the active sets at the solution are shown in Figure 6.

As one can observe in Figure 6, the constraint allows the solution to be quite steep on the boundary of Ω. Accordingly, the active sets are mainly inactive on the boundary - apart from a small region. Near the center of Ω, the constraint requires the solution to be very flat, which leads to a plateau in the solution at that region. The active sets are located mainly in those regions of Ω, where the length of the gradient is forced to decrease rapidly.

Correspondingly, one observes in Figure 7 that the gradients are quite steep near the boundary but very flat in the center. Because of the form of the right hand

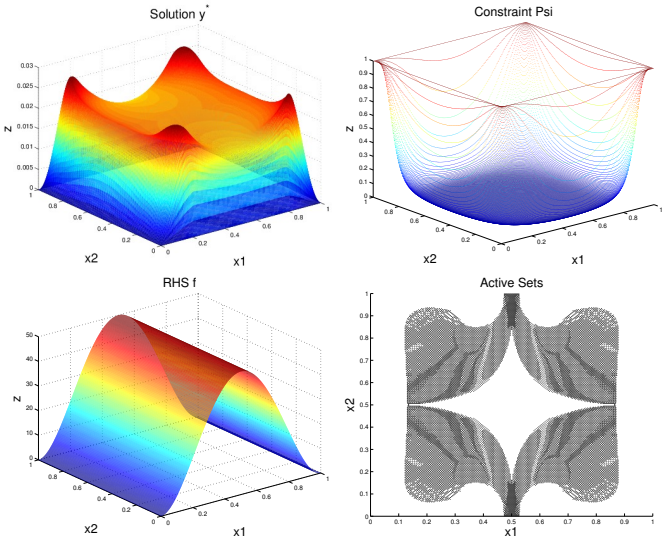

Figure 6. Optimal solution y^* (upper left plot), Constraint ψ (upper right plot), right hand side f (lower left plot) and the active sets (lower right plot, active sets plotted in black) for test problem P3 using (P^2_γ), i.e., p calculated exact, mesh size $h = \frac{1}{256}$.

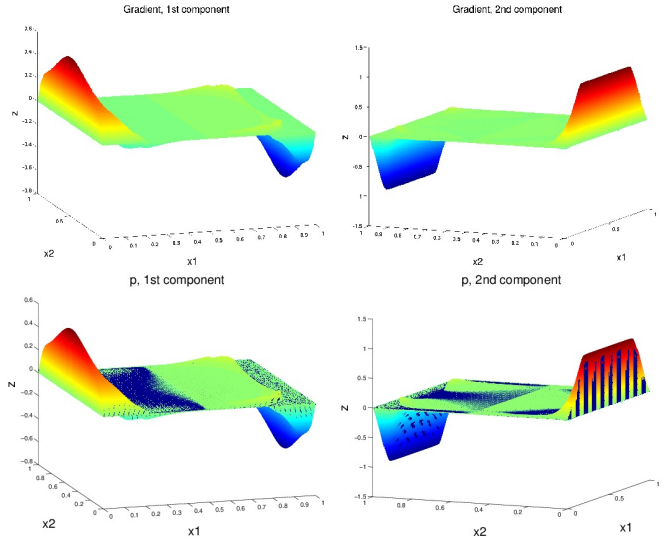

Figure 7. The first component of the gradient (upper left plot), the second component of the gradient (upper right plot), Parameter p (lower plots) for test problem P3 using (P^2_γ), i.e., p calculated exact, mesh size $h = \frac{1}{256}$.

side f, one can see here that the gradients are steeper with respect to x_2 than with respect to x_1. This explains the active regions on the upper and lower end of the active set plot in Figure 6. Exemplarily, we show here the gradients and p plots using method (P^2_γ) and again we observe an excellent fit of p approximating the gradient of the solution.

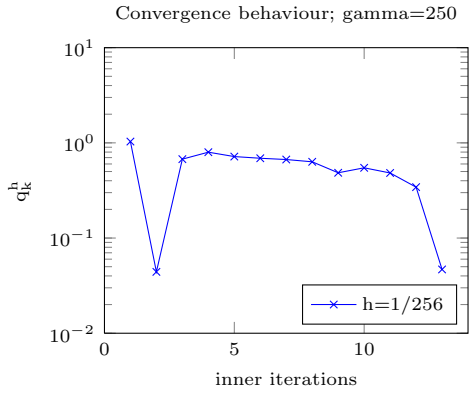

Figure 8. Discrete quotients q_k per inner iteration, mesh size $h = \frac{1}{256}$.

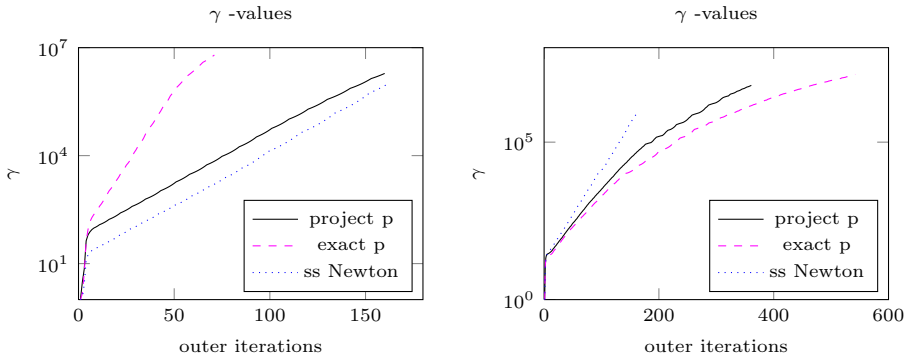

Figure 9. Gamma-Updates for exact (left plot) and inexact path-following (right plot), mesh size $h = \frac{1}{128}$.

Convergence Rate of the Semismooth Newton Method. We used problem P1 to test the convergence rate of the semismooth Newton method. Heuristically, we set $\gamma = 250$ fixed. Since y^* was analytically not available, the last iterate of an identical previous iteration performed with high accuracy was used. Here, the CG-method was stopped when the residual was smaller than 10^{-12}. In Figure 8 we plot the discrete versions of the quotients

$$q_k = \frac{\|y_{k+1} - y^*\|_{H_0^1(\Omega)}}{\|y_k - y^*\|_{H_0^1(\Omega)}}. \tag{5.1}$$

In Figure 8 one observes that after the iterations have leveled off, the convergence rate is linear, i.e. $q_k < 1$. Approaching the solution (roughly from iteration 10), the convergence rate becomes superlinear.

Gamma Update. In Figure 9 we depict the γ-updates for exact and inexact path-following using a logarithmic scale. As one can see for all methods, γ reaches values of at least 10^5.

Comparing Inner and Outer Iteration Numbers. Plotting the inner iteration numbers per outer iteration in case of exact path-following and inexact path-following (here exemplarily) for test problem P2 , we obtain the results shown

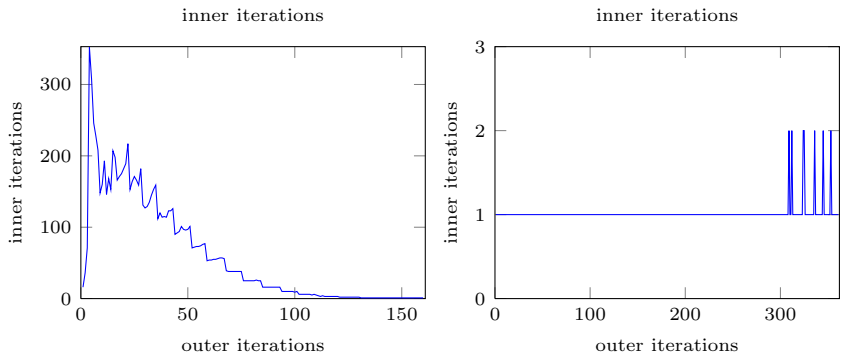

Figure 10. Number of iterations (vertical axis) per outer iteration for test problem P2 for exact path-following (left plot) and for inexact path-following (right plot) using (P^1_γ), i.e., p calculated via projection, mesh size $h = \frac{1}{128}$.

in Figures 10, 11 and 12. We note that the test runs for the other problems yielded qualitatively similar plots.

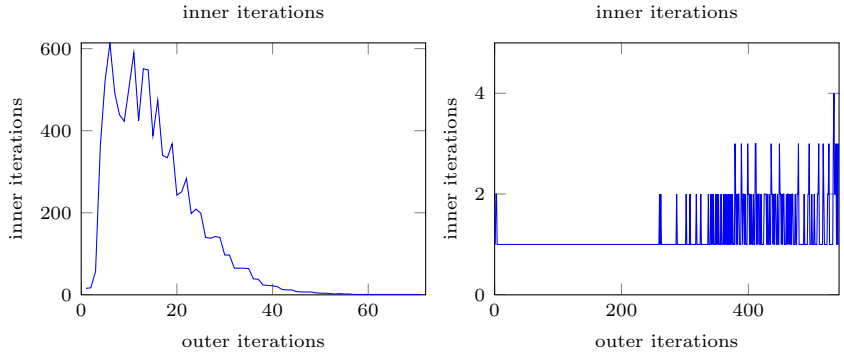

Figure 11. Number of iterations (vertical axis) per outer iteration for test problem P2 for exact path-following (left plot) and for inexact path-following (right plot) using (P^2_γ), i.e., p calculated exact, mesh size $h = \frac{1}{128}$.

All methods (except inexact path-following) stopped their respective inner iterations using $\epsilon_{inner} = 5 \cdot 10^{-7}$ as described in Section 2 resp. Section 3.3. To compare the results, the outer iterations were stopped using the same stopping criterion for all three approaches. In fact, for $\lambda(x)$ given according to the respective method we checked whether the system

$$
\begin{aligned}
&-\Delta y - f - \operatorname{div} \lambda q_{\nabla y} = 0 \text{ in } H^{-1}(\Omega) \\
&\lambda(x) \geq 0,\ |\nabla y(x)|_2 - \psi(x) \leq 0,\ \lambda(x)(|\nabla y(x)|_2 - \psi(x)) = 0 \text{ for a.e. } x \in \Omega,
\end{aligned}
$$

was satisfied. As shown for (P^1_γ) on p. 7, we choose $\lambda = \gamma(|\nabla y|_2 - \psi)$. Comparing the definition of F_γ on p. 9 with the equation above, it becomes apparent that we define λ in the same way as above in the case of the Newton solver. In case of exact

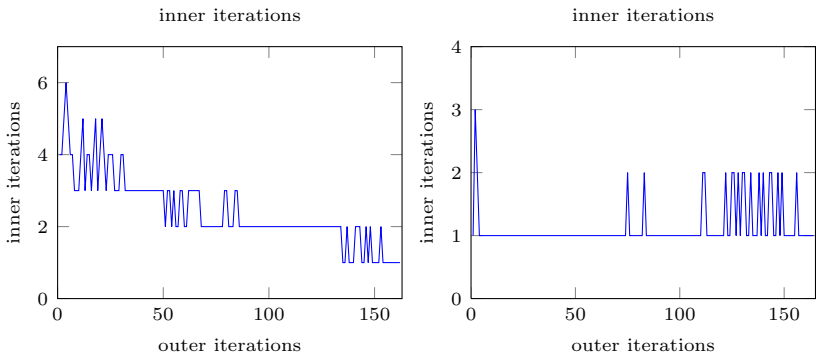

Figure 12. Number of iterations (vertical axis) per outer iteration for test problem P2 for exact path-following (left plot) and for inexact path-following (right plot) using (P^3_γ), i.e., using the semismooth Newton method, mesh size $h = \frac{1}{128}$.

p, as noted before, we use $\lambda = \frac{\gamma}{2}(|\nabla y|_2 - \psi)$. With this information at hand, we define

$$\begin{aligned} \mathrm{res}_6(y) &:= -\Delta y - f - \operatorname{div} \lambda q_{\nabla y}, \\ \mathrm{res}_7(y) &:= \lambda - \max\big(0, \lambda + c(|\nabla y|_2 - \psi)\big) \end{aligned}$$

and terminate the outer loop as soon as

$$\begin{aligned} \|\mathrm{res}_6(y_{\gamma_\ell})\|_{H^{-1}(\Omega)} &\leq (1 + \|\mathrm{res}_6(y_{\gamma_0})\|_{H^{-1}(\Omega)})\epsilon_{outer,1} \\ \|\mathrm{res}_7(y_{\gamma_\ell})\|_{L^2(\Omega)} &\leq (1 + \|\mathrm{res}_7(y_{\gamma_0})\|_{L^2(\Omega)})\epsilon_{outer,2} \end{aligned}$$

is fulfilled, for some $\epsilon_{outer,i} > 0$, $i = 1, 2$. We choose $\epsilon_{outer,2} = 10^{-6}$. Numerically, we cannot ensure that $p_k = p_{k+1}$ in cases of projected and exact p due to errors resulting from numerical approximations. We therefore relax the first stopping criterion by setting $\epsilon_{outer,1} = \max(10^{-5}, \gamma \|p_k - p_{k+1}\|_{L^2(\Omega)^n})$. Analogously, in case of (P^3_γ), i.e., the semismooth Newton solver, for numerical approximation reasons we cannot ensure $L(\nabla y_k)(\nabla y_{k+1} - \nabla y_k) = 0$. Hence, we use

$$\epsilon_{outer,1} = \max(10^{-5}, \gamma \|L(\nabla y_k)(\nabla y_{k+1} - \nabla y_k)\|_{L^2(\Omega)^n}).$$

Comparing the plots in Figures 10, 11 and 12 for exact path-following, we observe that for all methods the number of inner iterations decreases as the outer iterations proceed. This can be explained by the fact that the starting points get better with increasing γ such that the methods converge using less inner iteration steps. In case of inexact path-following, the methods require significantly less inner iterations. For the same reason, we need here more outer γ-update steps until convergence which can be seen in the Figures 10 and 11. In Figure 12 the number of outer iterations is similar. Overall, the semismooth Newton method needs very few (inner and outer) iterations only, when compared to the other methods. This is due to the rapid local convergence of our Newton scheme.

Exact vs. Inexact Path-Following. The dependence of the iteration number on the mesh size of the discretization (here exemplarily) for test problem P2 is depicted in Table 1 for (P^1_γ), in Table 2 for (P^2_γ) and in Table 3 for (P^3_γ) for exact and inexact path-following. The number of inner iterations is depicted in parenthesis. We note again that the test runs for the other test problems yielded qualitatively similar results.

	Mesh size h				
Version	1/16	1/32	1/64	1/128	1/256
EP	160(5973)	163(8327)	163(9111)	160(9688)	169(9775)
IP	328(656)	362(724)	367(770)	361(729)	378(768)

Table 1. Comparison of iteration counts for exact path-following (EP) and inexact path-following (IP) for different mesh sizes for test problem P2 using (P^1_γ), i.e., p calculated via projection: #outer iterations(#inner iterations)

	Mesh size h				
Version	1/16	1/32	1/64	1/128	1/256
EP	66(5702)	75(8824)	74(9605)	71(10208)	78(10156)
IP	457(916)	491(1065)	536(1259)	542(1199)	556(1222)

Table 2. Comparison of iteration counts for exact path-following (EP) and inexact path-following (IP) for different mesh sizes for test problem P2 using (P^2_γ), i.e., p calculated exact: #outer iterations(#inner iterations)

	Mesh size h				
Version	1/16	1/32	1/64	1/128	1/256
EP	164(486)	161(488)	163(518)	162(558)	165(624)
IP	213(435)	178(369)	187(389)	164(349)	163(396)

Table 3. Comparison of iteration counts for exact path-following (EP) and inexact path-following (IP) for different mesh sizes for test problem P2 using (P^3_γ), i.e. using the semismooth Newton method: #outer iterations(#inner iterations)

Overall, in case of inexact path following, one observes slightly more outer iterations and less inner iterations than in case of exact path following - corresponding to the observation above in p.23 ff. In case of exact path following, the method using the projected p and the semismooth Newton method require about the same outer iteration numbers. This is mirrored comparing these numbers with Figure 9 on p.23. Further, one observes in Figure 9 that the γ-values for these methods are essentially of the same size. The method using exact p seems to need fewer γ-updates. Figure 9 shows that the γ-values increase more rapidly. But because of the high number of inner iterations needed by the method, the overall iteration numbers are still higher than the ones of the semismooth Newton method. Comparing the numbers of outer iterations, then the results clearly indicate that the outer iterations are mesh independent. This shows that the techniques working in function spaces introduced here, result in an algorithmic framework which performs stably with respect to decreasing mesh size. As expected, the methods using projected p and exact p depicted in Tables 1 and 2 need in case of exact about ten times and for inexact path-following about three times more overall iterations than the semismooth Newton method depicted in Table 3. This demonstrates the significantly faster overall convergence of the semismooth Newton solver for exact path following. For inexact path-following there is a trade-off between the iteration number and CPU-times. In this vein we also note that each method, Algorithm 2.1, 2.3 and the semismooth Newton algorithm 3.2, requires to solve a second-order

linear elliptic partial differential equation, i.e. with respect to solution time all methods consume a similar CPU-time per iteration. However, while the operator (matrix) in Algorithm 2.1 and 2.3, respectively, is independent of the iteration (it only depends on γ), Newton's method exhibits an iteration dependent part of the linearized operator. This results in the necessity to re-assemble the associated part of the matrix (pertinent to γ). Consequently, one faces a computational overhead which is responsible for the trade-off in iterations and CPU time when comparing Algorithm 2.1, 2.3 and the semismooth Newton algorithm 3.2 in both, exact as well as inexact, settings. In the tests reported here the semismooth Newton method still outperformed the other algorithms with respect to CPU time. In order to further speed up Algorithm 2.1 and 2.3, respectively, one may factorize the respective iteration matrix and store the corresponding factor for every fixed γ.

6. Conclusions

In this paper we design and numerically analyze three different algorithmic approaches for minimizing the Dirichlet energy subject to pointwise constraints on the gradients of the state variable. Two methods are of variable splitting type, which is currently a popular technique in total variation regularization based image processing. These methods typically exhibit a linear convergence rate with their major appeal lying in the fact that their iterates can be determined explicitly by a closed formula or by solving a Poisson-type problem which is independent of the iterates (but depends on γ). The third method is of generalized Newton type. It has the advantage of local superlinear convergence at the expense of a system matrix which needs to be updated from iteration to iteration. All methods relax the pointwise gradient constraints in a different way. The relaxation depends on γ and induces a path-following scheme. We analyzed exact as well as practically more relevant inexact path-following methods. As expected, the latter requires a smaller number of linear system solves when compared to the exact variants. Comparing the three methods, we find that the variable splitting schemes require significantly more iterations than the Newton iterations, where the difference is more pronounced in case of exact path-following. In our tests, the trade-off between the number of linear system solves and the cost of re-assembling the system matrix is in favor of the generalized Newton scheme. However, we note that the splitting methods may still be sped up by specializing matrix factorizations. With respect to function space convergence we note that the Newton scheme hinges on a lifting step, whose explicit structure is not straight forward. In our numerics, however, we found that stable convergence under mesh refinements can be obtained even without such an additional lifting.

Future directions may involve a further analysis including the lifting step for the generalized Newton scheme, applying multigrid type preconditioners and exploiting sparse numerical linear algebra for further speed-ups in particular for the splitting schemes.

References

[1] Adams, R., and Fournier, J. *Sobolev Spaces*. No. 140 in Pure and Applied Mathematics. Academic Press, 2003.

[2] Alt, H. W. *Lineare Funktionalanalysis: Eine anwendungsorientierte Einführung*. Springer-Verlag, Berlin Heidelberg New York, 1992.

[3] Attouch, H., Buttazzo, G., and Michaille, G. *Variational Analysis in Sobolev Spaces and BV Spaces -Applications to PDEs and Optimization*. MPS-SIAM Series on Optimization.

Society for Industrial and Applied Mathematics (SIAM) and the Mathematical Programming Society (MPS), Philadelphia, PA, 2006.

[4] Barrett, J. W., and Prigozhin, L. A Quasi-Variational Inequality Problem in Superconductivity. *Mathematical Models and Methods in Applied Sciences 20*, 5 (2010), 679–706.

[5] Bonnans, J. F., and Shapiro, A. *Perturbation Analysis Of Optimization Problems*. Springer Series in Operations Research. Springer, New York Berlin Heidelberg, 2000.

[6] Brezis, H., and Sibony, M. Equivalence de deux inéquations variationelles et applications. *Archive Rat. Mech. Anal. 41* (1971), 254–265.

[7] Cherednichenko, S., Krumbiegel, K., and Rösch, A. Error estimates for the Lavrentiev regularization of elliptic optimal control problems. *Inverse Problems 24*, 5 (2008), 055003.

[8] Christensen, P. A nonsmooth newton method for elastoplastic problems. *Comput. Methods Appl. Mech. Engrg. 191* (2002), 1189–1219.

[9] Ekeland, I., and Témam, I. *Convex Analysis and Variational Problems*. Classics in Applied Mathematics. Society for Industrial and Applied Mathematics (SIAM), Philadelphia, 1999.

[10] Glowinski, R., Lions, J.-L., and Trémolières, R. *Numerical Analysis of Variational Inequalities*. No. 8 in Studies in Mathematics and its Applications. North-Holland Publishing Company, Amsterdam, New York, Oxford, 1981.

[11] Gröger, K. A $W^{1,p}$-Estimate for Solutions to Mixed Boundary Value Problems for Second Order Elliptic Differential Equations. *Mathematische Annalen 283* (1989), 679–687.

[12] Gruber, P., and Valdman, J. Solution of one-time-step problems in elastoplasticity by a slant newton method. *SIAM Journal on Scientific Computing 31*, 2 (2009), 1558–1580.

[13] Hintermüller, M., and De los Reyes, J.-C. A duality-based semismooth newton framework for solving variational inequalities of the second kin. *Interfaces and Free Boundaries 13* (2011), 437–462.

[14] Hintermüller, M., Ito, K., and Kunisch, K. The Primal-dual Active Set Strategy As A Semismooth Newton Method. *SIAM Journal on Optimization 13*, 3 (2003), 865–888.

[15] Hintermüller, M., and Kunisch, K. Path-following Methods For A Class Of Constrained Minimization Problems in Function Space. *SIAM Journal on Optimization 17*, 1 (2006), 159–187.

[16] Hintermüller, M., and Kunisch, K. PDE-Constrained Optimization Subject to Pointwise Constraints on the Control, the State, and Its Derivative. *SIAM Journal on Optimization 20*, 3 (2009), 1133–1156.

[17] Hintermüller, M., and Rautenberg, C. A Sequential Minimization Technique for Elliptic Quasi-Variational Inequalities with Gradient Constraints. *SIAM Journal on Optimization 22*, 4 (2012), 1224–1257.

[18] Hintermüller, M., and Rösel, S. A duality-based path-following semismooth newton method for elasto-plastic contact problems. IFB-Report 70, Karl-Franzens Universität Graz, Heinrichstrasse 36, A-8010 Graz, Austria, 09 2013.

[19] Hintermüller, M., Schiela, A., and Wollner, W. The length of the primal-dual path in moreau-yosida-based path-following for state-constrained optimal control. *SIAm J. Optimization 24*, 1 (2014), 108–126.

[20] Hintermüller, M., and Ulbrich, M. A Mesh-independence Result for Semismooth Newton Methods. *Mathematical Programming 101*, 1 (2004), 151–184.

[21] Ioffe, A., and Tihomirov, V. *Theory of Extremal Problems*. North-Holland Publishing Company, Amsterdam, New York, Oxford, 1979.

[22] Ito, K., and Kunisch, K. Semi-smooth Newton Methods For Variational Inequalities Of The First Kind. *ESIAM: M2AN 37*, 1 (2003), 41–62.

[23] Ito, K., and Kunisch, K. *Lagrange Multiplier Approach to Variational Problems and Applications*. Advances in Design and Control. Society for Industrial and Applied Mathematics (SIAM), Philadelphia, PA, 2008.

[24] Kunze, M., and Rodrigues, J. F. An Elliptic Quasi-Variational Inequality with Gradient Constraints and some of its Applications. *Mathematical Methods in the Applied Sciences 23* (2000), 897–908.

[25] Schiela, A. An interior point method in function space for the efficient solution of state constrained optimal control problems an interior point method in function space for the efficient solution of state constrained optimal control problems. *Math. Prog. 138*, 1 (2013), 83–114.

[26] Schiela, A., and Wollner, W. Barrier methods for optimal control problems with convex nonlinear gradient state constraints. *SIAm J. Optimization 21*, 1 (2011), 269–286.

[27] Stadler, G. *Infinite-dimensional Semi-smooth Newton and Augmented Lagrangian Methods for Friction and Contact Problems in Elasticity*. PhD thesis, Karl-Franzens University of Gray, 2004.

[28] Tröltzsch, F. Regular Lagrange multipliers for control problems with mixed pointwise control-state constraints. *SIAM J. Optimization 15*, 2 (2005), 616–634.
[29] Tröltzsch, F., Prüfert, U., and Weiser, M. The convergence of an interior point method for an elliptic control problem with mixed control-state constraints. *Computational Optimization and Applications 39*, 2 (2008), 183–218.
[30] Ulbrich, M., and Ulbrich, S. Primal-dual interior-point methods for PDE-constrained optimization. *Math. Prog. 117* (2009), 435–485.
[31] Wieners, C. Nonlinear solution methods for infinitesimal perfect plasticity. *Z. Angew. Math. Mech. 87*, 8-9 (2007), 643–660.
[32] Wloka, J. *Partielle Differentialgleichungen*. Teubner, Stuttgart, 1982.

Institut für Mathematik, Humboldt-Universität zu Berlin, Berlin, Germany

E-mail address: hint@math.hu-berlin.de, rasch@math.hu-berlin.de